Residual Water Modulates Q_A^--to-Q_B Electron Transfer in Bacterial Reaction Centers Embedded in Trehalose Amorphous Matrices

Francesco Francia,* Gerardo Palazzo,† Antonia Mallardi,‡ Lorenzo Cordone,§ and Giovanni Venturoli*¶

*Laboratorio di Biochimica e Biofisica, Dipartimento di Biologia, Università di Bologna, Bologna, Italy; †Dipartimento di Chimica, Università di Bari, Bari, Italy and Dipartimento di Scienze e Tecnologie Agro-alimentari Ambientali e Microbiologiche, Università del Molise, Campobasso, Italy; ‡Istituto per i Processi Chimico-Fisici, Consiglio Nazionale delle Recerche, Bari, Italy; §Dipartimento di Scienze Fisiche ed Astronomiche and Istituto Nazionale per la Fisica della Materia, Palermo, Italy; and ¶Istituto Nazionale per la Fisica della Materia, Unità di Ricerca di Bologna, Bologna, Italy

ABSTRACT The role of protein dynamics in the electron transfer from the reduced primary quinone, Q_A^-, to the secondary quinone, Q_B, was studied at room temperature in isolated reaction centers (RC) from the photosynthetic bacterium *Rhodobacter sphaeroides* by incorporating the protein in trehalose water systems of different trehalose/water ratios. The effects of dehydration on the reaction kinetics were examined by analyzing charge recombination after different regimes of RC photoexcitation (single laser pulse, double flash, and continuous light) as well as by monitoring flash-induced electrochromic effects in the near infrared spectral region. Independent approaches show that dehydration of RC-containing matrices causes reversible, inhomogeneous inhibition of Q_A^--to-Q_B electron transfer, involving two subpopulations of RCs. In one of these populations (i.e., *active*), the electron transfer to Q_B is slowed but still successfully competing with $P^+Q_A^-$ recombination, even in the driest samples; in the other (i.e., *inactive*), electron transfer to Q_B after a laser pulse is hindered, inasmuch as only recombination of the $P^+Q_A^-$ state is observed. Small residual water variations (~7 wt %) modulate fully the relative fraction of the two populations, with the active one decreasing to zero in the driest samples. Analysis of charge recombination after continuous illumination indicates that, in the inactive subpopulation, the conformational changes that rate-limit electron transfer can be slowed by >4 orders of magnitude. The reported effects are consistent with conformational gating of the reaction and demonstrate that the conformational dynamics controlling electron transfer to Q_B is strongly enslaved to the structure and dynamics of the surrounding medium. Comparing the effects of dehydration on $P^+Q_A^-\rightarrow PQ_A$ recombination and $Q_A^-Q_B\rightarrow Q_AQ_B^-$ electron transfer suggests that conformational changes gating the latter process are distinct from those stabilizing the primary charge-separated state.

INTRODUCTION

Proteins display an extremely large number of conformational substates, which at physiological temperatures are reflected in complex conformational dynamics, intimately connected to protein reactivity (Frauenfelder et al., 1988, 1991; Frauenfelder and Wolynes, 1994, Frauenfelder and McMahon, 1998). The activation of this protein dynamics coupled to biological functionality appears to require a minimum water content (see e.g., Careri, 1992; Barron et al., 1997; Mattos, 2002). The possibility that internal motions determine the rate of long-range electron transfer catalyzed by redox proteins is well-recognized (see e.g., Hoffman and Ratner, 1987; Davidson, 1996; Kotelnikov et al., 1998; Sharp and Chapman, 1999; Balabin and Onuchic, 2000; Cherepanov et al., 2001). These motions, in principle, cover a wide temporal window (from femtoseconds to seconds), extending from fast vibrations of atoms to slow displacements of large protein domains (Woodbury and Parson, 1986; Peloquin et al., 1994; McMahon et al., 1998; Zhang et al., 1998; Izrailev et al., 1999).

The photosynthetic reaction center (RC) from purple bacteria, allowing the study of single-turnover reactions initiated by a pulse of light, provides an excellent laboratory for exploring the relationship between protein dynamics and electron transfer events. This integral pigment-protein complex catalyzes a light-induced charge separation across the membrane dielectric, thus promoting the primary event of photosynthetic energy transduction (Gunner, 1991). Within the photosynthetic RC from *Rhodobacter sphaeroides* a bacteriochlorophyll dimer (P) acts as the primary electron donor: after absorption of a photon, it delivers an electron (via a bacteriopheophytin molecule) to the primary ubiquinone acceptor Q_A, generating the primary charge-separated state $P^+Q_A^-$. The photo-reduced Q_A^- in turn reduces a ubiquinone-10 molecule bound at the secondary acceptor Q_B site. When no physiological or artificial electron donor is available to re-reduce P^+, the electron on Q_B^- recombines with the hole on P^+, restoring the initial ground state of the RC (Feher et al., 1989; Okamura et al., 2000).

Several independent experimental findings point toward structural changes accompanying light-induced charge separation within the reaction center (Arata and Parson, 1981; Woodbury and Parson, 1984; Kleinfeld et al., 1984a; Kirmaier et al., 1985; Parot et al., 1987; Nabedryk et al., 1990; Brzezinski and Andreasson, 1995; Kalman and Maroti, 1997; Stowell et al., 1997; Edens et al., 2000). The more direct evidences of a close coupling between electron transfer and protein conformational dynamics were obtained by comparing the rate of specific electron transfer processes

Submitted February 12, 2003, and accepted for publication July 23, 2003.

Address reprint requests to Giovanni Venturoli, E-mail: ventur@alma.unibo.it.

0006-3495/03/10/2760/16 $2.00

in RCs frozen in the dark and under illumination. These pioneering studies have shown that RCs can be trapped at cryogenic temperatures in dark-adapted and light-adapted conformations drastically differing in the stability of the primary charge-separated state $P^+Q_A^-$ (Kleinfeld et al., 1984a); both these conformations consist of distribution of substates which result in a wide spectrum of electron transfer rates for charge recombination of the $P^+Q_A^-$ state (Kleinfeld et al., 1984a, McMahon et al., 1998). A second reaction, which has been intensively investigated in relation to RC dynamics, is the electron transfer from the primary reduced to the secondary ubiquinone acceptor. When RCs are frozen in the dark at temperatures <200 K, the electron transfer from Q_A^- to Q_B stops; by contrast, it persists even at 50 K in RC frozen under illumination and then allowed to return to the ground state (Kleinfeld et al., 1984a, Xu and Gunner, 2001). Consistently, at room temperature, the rate of electron transfer between the primary and secondary quinone was found to be independent of the associated redox free energy change (Graige et al., 1998). Such an independence of the driving force indicates that the reaction is not rate-limited by electron transfer itself, but gated by some other process. The reaction appears to be limited by proton binding at high pH (>8.0) and by conformational changes at pH < 8.0 (Paddock et al., 1989; Takahashi and Wraight, 1992; Xu and Gunner, 2002). Moreover, it has been shown that, at 120 K < T < 200 K, RCs frozen under illumination can relax to a Q_A^--to-Q_B inactive conformation, which is different from the dark-adapted one (Xu and Gunner, 2001). Recent temperature-dependence studies are beginning to shed some light on the complex energy landscape that governs this electron transfer process (Xu and Gunner, 2002; Xu et al., 2002).

Function-dynamics coupling is usually studied by hampering protein substate interconversion and relaxations at cryogenic temperatures (Austin et al., 1975; Ortega et al., 1996; McMahon et al., 1998). Alternatively, a severe conditioning of the internal protein dynamics can be achieved at room temperature by embedding the protein within a saccharide matrix and by dehydrating the resulting sample. In particular, the relationship between function and dynamics has been studied extensively by incorporating heme-proteins into dry trehalose glassy matrices (Hagen et al., 1995, 1996; Gottfried et al., 1996; Librizzi et al., 2002). Trehalose, a disaccharide found in large amounts in organisms that can survive conditions of extreme dehydration and high temperature, also exhibits peculiar properties in the preservation of biostructures (see e.g., Leslie et al., 1995; Uritani et al., 1995; Crowe et al., 1996). In trehalose matrices, nonharmonic contributions to internal motions (called protein-specific motions) are severely hindered, as shown by Mössbauer and optical absorption spectroscopy, neutron scattering, and molecular dynamics simulations (Cordone et al., 1998, 1999; Cottone et al., 2001). The analysis of function-dynamics coupling in trehalose matrices of different water content, at room temperature, offers a distinctive opportunity in relation to temperature-dependence studies performed at cryogenic temperatures: this approach in fact uncouples temperature from solvent effects. In principle, it can yield better insights on the extent to which protein internal dynamics is enslaved to the structure and dynamics of the external medium (Vitkup et al., 2000).

It has been reported that for carboxy myoglobin embedded in trehalose matrices of decreasing water content, the interconversion among conformational substates is progressively blocked at room temperature (Librizzi et al., 1999, 2002). In full agreement, we have recently shown that bacterial photosynthetic RCs can be functionally incorporated into trehalose matrices and that trehalose coating can be used to condition protein dynamics coupled to electron transfer in this large integral membrane protein (Palazzo et al., 2002). In extensively dehydrated trehalose matrices, RC relaxation from the dark-adapted to the light-adapted conformation and interconversion between conformational substates could be blocked at room temperature over the timescale of hundreds of milliseconds: the impairment was reflected in inhomogeneous kinetics of $P^+Q_A^-$ charge recombination. In the present work we exploited a similar strategy to assess the role of conformational dynamics in electron transfer from the primary photo-reduced (Q_A^-) to the secondary (Q_B) quinone acceptor. The reaction has been investigated by studying the kinetics of charge recombination after a laser pulse in progressively dehydrated trehalose matrices. We show that Q_A^--to-Q_B electron transfer can be slowed down by orders of magnitude at room temperature when the water content of the trehalose matrix is decreased over a limited range. By examining the kinetics of charge recombination after periods of continuous illumination the time course of the relaxation processes which control electron transfer has been determined as a function of the residual water.

MATERIALS AND METHODS

The RCs were isolated and purified from *Rb. sphaeroides* R-26 according to Gray et al. (1990). This isolation procedure gives RCs with a Q_B content/activity of ~50%. Reconstitution of the secondary quinone acceptor was achieved as in van Mourik et al. (2001) with minor changes, as described below. The purified RC was loaded on a column of DE-52 (Whatman, Maidstone, UK) previously equilibrated with buffer Tris-HCl 20 mM pH 8, 0.025% lauryl dimethylamine-*n*-oxide (LDAO) containing ubiquinone-10 (UQ-10; from Sigma Chemical, St. Louis, MO). The low solubility of UQ-10 in aqueous buffer was overcome by adding the quinone to the 30% LDAO stock solution used for preparing buffer. The RCs were extensively washed with the same buffer, eluted with 400 mM NaCl and dialyzed overnight. Q_B activity of the reconstituted samples was typically >95%.

Trehalose was from Hayashibara Shoij (Okayama, Japan). The concentration of trehalose in the samples is reported as trehalose weight percent (wt %), i.e.: (*grams of trehalose*/*grams of trehalose plus water*) %, neglecting the contribution of RC, buffer, and detergent to the sample weight.

Liquid samples (16 wt % and 53 wt % trehalose) were prepared by dissolving suitable amounts of trehalose in aqueous buffer (5 mM Tris pH = 7.5; 0.025% LDAO); the RC was added to this sugar solution from the

concentrated stock solution. The sample composition was evaluated by weight.

Plasticized amorphous and glassy samples were prepared by drying under N_2 flow a thin layer of a trehalose solution containing RC on optical glass plates, as described in detail in Palazzo et al. (2002). Data were collected at 298 K at various times during the drying of trehalose matrices kept under dry nitrogen atmosphere.

The water content of the amorphous matrices was assayed by visible and near infrared (NIR) spectroscopy on a PerkinElmer (Fremont, CA) Lambda 19 spectrometer. To estimate the relative sample composition, the area of the combination band of water at 1950 nm was considered and the RC absorption at 802 nm was used as an internal standard (Palazzo et al., 2002).

Rapid absorbance changes were monitored with a spectrophotometer of local design (Mallardi et al., 1997). RC photochemistry was elicited by a 20-ns pulse from a dye-laser (RDP-1; Radiant Dyes GmbH, Wermelskirchen, Germany) pumped by a frequency-doubled *Q*-switched Nd-YAG laser (Surelite 10, Continuum, Santa Clara, CA). Stryryl 9 was used as a dye (λ_{max} at 810 nm); only in double flash experiments, to increase pulse saturation, sulphorhodamine B was used (λ_{max} = 590 nm). The kinetics of charge recombination were monitored at 605 nm, 450 nm, and 422 nm (Feher and Okamura, 1978). The photomultiplier was protected from scattered excitation light by 0.01% blocking, 10-nm bandwidth interference filters centered at the corresponding wavelengths. Electrochromic transients associated with Q_A^--to-Q_B electron transfer were measured in the 750-nm region (Vermeglio and Clayton, 1977); in these measurements the photomultiplier was protected by a monochromator plus an interference filter. Continuous illumination was provided by a 200-W quartz tungsten halogen lamp collimated by an optical condenser and filtered by 8 cm of thermostated water and by a colored glass long-pass filter with a cut-on wavelength of 780 nm. In continuous illumination experiments we used a Uniblitz electro-programmable shutter system, characterized by a 3-ms closure time (Vincent Associates, Rochester, NY).

Nonlinear least-squares minimization was performed by computer routines based on a modified Marquardt algorithm (Bevington, 1969). Confidence intervals of fitting parameters were estimated numerically by an exhaustive search method (Beechem, 1992; Holzwarth, 1996). The confidence interval was obtained by using an F-statistics routine to determine the probability of a particular fractional increase in chi-square, as described in Palazzo et al. (2002).

RESULTS AND DISCUSSION

Charge recombination in trehalose solutions and amorphous matrices

When isolated RCs are activated by a flash of light, the state $P^+Q_A^-Q_B$ is formed in <200 ps. Subsequent electron transfer events can be suitably described by the following equation:

$$PQ_AQ_B \xleftarrow{k_{AP}} P^+Q_A^-Q_B \underset{k_{BA}}{\overset{k_{AB}}{\rightleftharpoons}} P^+Q_AQ_B^- \qquad (1)$$
$$\uparrow \_\_\_\_\_ \downarrow$$
$$k_{BP}$$

The state $P^+Q_A^-Q_B$ can either recombine yielding the ground state PQ_AQ_B with a rate constant $k_{AP} \cong 10\ s^{-1}$ or, in the presence of ubiquinone bound at the Q_B site, yield $P^+Q_AQ_B^-$. Under physiological conditions, the state $P^+Q_AQ_B^-$ is stabilized with respect to $P^+Q_A^-Q_B$ by ~70 meV and, since $(k_{AB} + k_{BA}) \cong 10^4\ s^{-1} \gg k_{AP}$, electron transfer to Q_B occurs with an extremely high quantum efficiency (Kleinfeld et al., 1984b). The state $P^+Q_AQ_B^-$ recombines slowly (lifetime ≅ 1 s) essentially via the $P^+Q_A^-Q_B$ state, with the direct route (k_{BP}) being negligible at room temperature (Kleinfeld et al., 1984b; Labahn et al., 1995). By contrast, the fast recombination of $P^+Q_A^-Q_B$ (lifetime ≅ 0.1 s) is observed whenever electron transfer to Q_B is blocked over this timescale. In general, since the quantum yield for Q_B^- formation and the consequent kinetics of recombination depend on k_{AB} and k_{BA} values relative to k_{AP}, information on the kinetics of electron transfer to Q_B can be obtained by following the kinetics of P^+ decay after a flash of light (Kleinfeld et al., 1984b; Mancino et al., 1984). We have used primarily this approach to examine the kinetics of Q_A^--to-Q_B electron transfer in trehalose solutions and plasticized or solid matrices.

Fig. 1 shows the room temperature kinetics of charge recombination after laser excitation for RC in trehalose solutions (Fig. 1 *A*) and matrices progressively dehydrated (Fig. 1 *B*). Even in solution and in the absence of trehalose (Fig. 1 *A*), the decay of P^+ is not strictly mono-exponential. A small fraction (≅ 5%) of P^+ decaying in the tens of ms timescale (i.e., undergoing $P^+Q_A^-$ recombination) is present. Moreover, the dominating slow component slightly deviates from an exponential decay, suggesting a relatively narrow continuous distribution of rate constants. In fact, this slow kinetic phase can be accurately analyzed by a cumulant expansion truncated at the second term (Palazzo et al., 2000). Accordingly, an adequate and physically meaningful function fitting the P^+ decays measured in liquid solutions, both in the presence and in the absence of trehalose, is (Ambrosone et al., 2002),

$$P^+(t)/P^+(0) = A_f \exp(-k_f \times t) + (1 - A_f) \times \exp\left(- \langle k_s \rangle t + \frac{1}{2}\sigma_s^2 \times t^2 \right), \qquad (2)$$

where A_f and $(1 - A_f)$ are the fractions of fast and slow decay, respectively; k_f is the rate constant of the fast component; and $\langle k_s \rangle$ and σ_s are the average rate constant and distribution width for the slow decaying component. When fitting the kinetics recorded in solution, we fixed the rate constant of the fast phase to 8.2 s^{-1} as measured for $P^+Q_A^-$ recombination in solution (Palazzo et al., 2002). This was done to avoid the effects of strong parameter correlation and in view of the low amplitude of the fast kinetic component. The validity of such an approach is confirmed by the fact that leaving k_f as an adjustable parameter yields values ranging between 8 s^{-1} and 10 s^{-1}, although with large uncertainty.

In liquid trehalose solutions, up to 53 wt %, the fraction of the slow phase, A_s, is essentially unchanged. However, the corresponding average rate constant, $\langle k_s \rangle$, decreases from ~0.7 s^{-1} in the absence of trehalose to 0.5 s^{-1} at 53 wt % trehalose (Fig. 1 *A*).

Drying (~10 h) under N_2 flow of a suitable protein-trehalose-detergent solution (see Materials and Methods) layered on an optical glass plate results in an amorphous

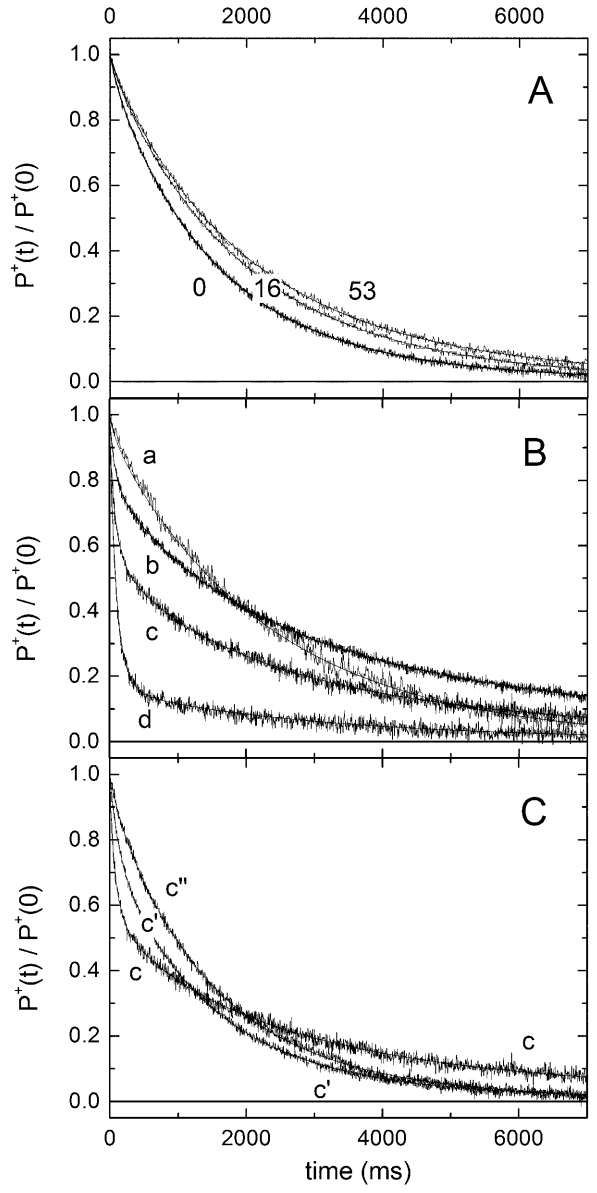

FIGURE 1 Kinetics of charge recombination after flash excitation of RCs in trehalose solutions and matrices. (*A*) Normalized P^+ decay after a flash at increasing trehalose concentrations (traces from *bottom* to *top*) in liquid samples. Labels indicate percent weight in trehalose. Continuous curves are best fit to Eq. 2, in which k_f was fixed to 8.2 s^{-1} (see text for details). Kinetic parameters are given in the following; values in parentheses represent the extremes of confidence intervals within two standard deviations (see Materials and Methods). 0 wt %: $A_f = 6.5\%$ (5.5, 7.5); $\langle k_s \rangle = 0.647$ s^{-1} (0.641, 0.653); and $\sigma_s = 0.14$ s^{-1} (0.12, 0.16). 16 wt %: $A_f = 4.4\%$ (2.1, 5.7); $\langle k_s \rangle = 0.518$ s^{-1} (0.512, 0.523); and $\sigma_s = 0.12$ s^{-1} (0.11, 0.13). 53 wt %: $A_f = 3.9\%$ (2.4, 5.5); $\langle k_s \rangle = 0.49$ s^{-1} (0.48, 0.50); and $\sigma_s = 0.15$ s^{-1} (0.14, 0.16). (*B*) Charge recombination kinetics in trehalose matrices at increasing degree of dehydration (traces *a–d*). Trace *a* was recorded in a ''wet'' matrix, in a state very close to the glass transition (trehalose concentration = 90 wt %). Trehalose concentrations of 94.3%, 95.4%, and 96.2% were evaluated by NIR spectroscopy (see Materials and Methods) in matrices *b*, *c*, and *d*, respectively. Continuous curves are best fit according to Eq. 4. The corresponding kinetic parameters are given in Table 1. (*C*) Effects of rehydration of a trehalose glass on the kinetics of P^+ decay. Trace *c*, solid matrix (95.4 wt % trehalose); trace *c′*, after resuspension (liquid sample, plasticized, transparent sample, which still contains residual loosely bound water that can be gradually removed by further drying under nitrogen (Palazzo et al., 2002). In the more ''wet'' matrix, obtained after ~10 h drying (Fig. 1 *B*, trace *a*), the kinetics of P^+ decay is similar to that observed in solution at high trehalose concentration (compare to Fig. 1 *A*). In such samples the slow decay fraction is essentially unchanged whereas the average rate constant $\langle k_s \rangle$ further decreases to 0.4 s^{-1} (Table 1). Resuspension of this ''wet'' sample fully restores the kinetic parameters measured in the corresponding initial (16 wt %) trehalose solution (compare to Fig. 1 *A* and Table 1). A more prolonged exposure to N_2 atmosphere results in larger dehydration (Fig. 1 *B* and Table 1, samples *b–d*). The trehalose concentration in such samples, estimated on the basis of the water absorption at ~1950 nm (Palazzo et al., 2002), increases from 94.3 wt % to 96.2 wt %. The progressive dehydration brings about a progressive increase of the amplitude of the fast component (A_f) of P^+ decay, corresponding to $P^+Q_A^-$ recombination. This component accounts for >80% of the decay in the driest sample (Fig. 1 *B* and Table 1, sample *d*), thus suggesting that dehydration impairs electron transfer from Q_A^- to Q_B in a substantial fraction of the RC population. Moreover, nonexponential decay becomes evident for both fast and slow kinetic components: a reasonable description of the P^+ decay requires two rate distributions (fast and slow). Accordingly, the kinetics can be fitted to either the sum of two cumulant expansions (Eq. 3), or the sum of two ''power laws'' (Eq. 4),

$$P^+(t)/P^+(0) = (1 - A_s)\exp\left(-\langle k_f\rangle t + \frac{1}{2}\sigma_f^2 t^2\right) + A_s \exp\left(-\langle k_s\rangle t + \frac{1}{2}\sigma_s^2 t^2\right) \quad (3)$$

$$P^+(t)/P^+(0) = (1 - A_s)/(1 + \lambda_f \times t)^{n_f} + A_s/(1 + \lambda_s \times t)^{n_s}, \quad (4)$$

where the subscripts *f* and *s* identify the fast and slow components. Parameters λ and *n* in Eq. 4 are related to $\langle k \rangle$ and σ in Eq. 3 by the following equations:

$$\langle k \rangle = n\lambda, \quad \sigma^2 = n\lambda^2. \quad (5)$$

Equations 3 and 4 fit the kinetics measured in dry samples equally well and yield comparable values of $\langle k \rangle$ and σ of the rate distribution functions, as was found in the analysis of $P^+Q_A^-$ recombination in dehydrated trehalose matrices (Palazzo et al., 2002). The fast kinetic component is constantly faster in dry samples than in solutions (average rate constant, $\langle k_f \rangle$, ranging between 11 s^{-1} and 14 s^{-1}) (Table 1). This acceleration is quantitatively consistent with

~16 wt % trehalose); and trace *c*,″ resuspended sample plus 60 μM ubiquinone-10 in LDAO (final detergent concentration 0.06%).

TABLE 1 Kinetic parameters of charge recombination in glassy matrices at increasing degree of dehydration

Sample	A_s	$\langle k_s \rangle$ (s^{-1})	σ_s (s^{-1})	$\langle k_f \rangle$ (s^{-1})	σ_f (s^{-1})
a					
Glass	0.94 (0.93, 0.96)	0.43 (0.42, 0.44)	0.18 (0.10, 0.24)	8.2	–
Resuspended	0.93 (0.92, 0.95)	0.50 (0.49, 0.51)	0.16 (0.14, 0.18)	8.2	–
b					
Glass	0.79 (0.78, 0.80)	0.39 (0.38, 0.40)	0.27 (0.16, 0.29)	12.7 (10.9, 15.0)	4.6 (0.2, 8.5)
Resuspended	0.96 (0.95, 0.97)	0.72 (0.71, 0.73)	0.26 (0.22, 0.28)	8.2	–
c					
Glass	0.54 (0.48, 0.56)	0.41 (0.36, 0.45)	0.24 (0.19, 0.29)	14.2 (11.2, 19.6)	5.6 (2.0, 9.4)
Resuspended	0.78 (0.77, 0.79)	0.71 (0.70, 0.72)	0.23 (0.22, 0.24)	8.2	–
Resuspended +UQ-10	0.94 (0.92, 0.95)	0.67 (0.66, 0.68)	0.19 (0.18, 0.20)	8.2	–
d					
Glass	0.16 (0.14, 0.19)	0.37 (0.27, 0.53)	0.18 (0.06, 0.38)	11.5 (10.0, 13.2)	4.5 (0.8, 7.4)
Resuspended	0.47 (0.44, 0.49)	0.88 (0.83, 0.93)	0.28 (0.23, 0.32)	8.2	–
Resuspended +UQ-10	0.90 (0.86, 0.93)	0.83 (0.80, 0.85)	0.28 (0.26, 0.30)	8.2	–

Samples are identified as in Fig. 1. Values obtained in the dehydrated glass, upon resuspension and after addition of ubiquinone-10 in LDAO, are compared for the different samples. Fitting to the sum of two rate distributions was performed according to Eqs. 4 and 5; other fitting procedures are described in detail in the text. Values in parentheses correspond to the extremes of the confidence interval within two standard deviations (see Materials and Methods).

that observed for the kinetics of $P^+Q_A^-$ recombination in Q_B-deprived RCs embedded in progressively dehydrated trehalose matrices (Palazzo et al., 2002). Rate constants ranging between 10 s^{-1} and 14 s^{-1} were obtained at a moderate dehydration, corresponding to trehalose concentrations between 92 wt % and 96 wt % (Palazzo et al., 2002), in line with NIR estimation of the water content of the present samples. The average rate constant of the residual slow phase, $\langle k_s \rangle$, does not change over this range of dehydration, remaining close to the value of 0.4 s^{-1} measured in the more ''wet'' amorphous matrix (Table 1).

The reversibility of the above effects was tested by redissolving samples at different degrees of drought (Fig. 1 *C* and Table 1). Equation 2, i.e., the same function used to describe kinetics in the initial trehalose solutions, was fitted to the kinetics of P^+ decay in redissolved samples. Upon resuspension of non-extremely dried samples a complete recovery of the amplitude of the slow kinetic component (A_s) is observed (e.g., sample *b* in Table 1). Correspondingly, the average rate constant of the slow phase, $\langle k_s \rangle$, which is 0.4 s^{-1} in dry samples, upon resuspension increases to 0.7 s^{-1}, indicating a full recovery of the kinetic behavior measured in solution before drying. However, samples exposed longer to dry N_2 atmosphere exhibit, after resuspension, only partial recovery of the amplitude of the slow kinetic component (see Fig. 1 *C*, trace *c′*, and Table 1, samples *c* and *d*). Based on the fact that Eq. 2, with k_f fixed at 8.2 s^{-1}, fits the kinetics in the redissolved samples well, one can infer that the effects of dehydration on $P^+Q_A^-$ recombination kinetics are fully reversible even in exhaustively dried samples. Analogous behavior has been observed in RC deprived of Q_B (Palazzo et al., 2002). The simplest explanation for the incomplete recovery of the slow component of P^+ decay upon resuspension of the more dehydrated matrices is that, during prolonged exposition to dry N_2 atmosphere, an unknown electron donor reduces Q_B to Q_BH_2 in a fraction of the RCs. This population lacking oxidized secondary acceptor will undergo only primary charge separation ($P^+Q_A^-$) and fast recombination. Several lines of evidence confirm this hypothesis:

- Partial reduction to UQH_2 can be assessed by spectrophotometry when detergent trehalose suspensions of ubiquinone-10, in the absence of the RC, are extensively dehydrated by prolonged (from 3 to 7 days) exposure to dry N_2 atmosphere and are successively fully rehydrated (spectra are shown in Supplemental Material). An absorbance increase at ~290 nm (diagnostic of UQH_2) is detected also upon resuspension of samples obtained by drying the detergent suspension under N_2 flux in the absence of trehalose (not shown);
- Analogous results are obtained with ubiquinone-0; in this case a larger fraction of ubiquinone is reduced upon exposure to N_2 (see spectra in Supplemental Material);
- Addition of an oxidant (1 mM $K_3[Fe(CN)_6]$), after resuspension of extensively dehydrated trehalose glasses, increases the relative amplitude of the slow phase of P^+ decay (not shown);
- When the exposure of the sample to N_2 is limited to a few hours and further dehydration is obtained under vacuum, a larger recovery of the slow kinetic component of charge recombination is observed upon rehydration of the solid matrix (not shown);
- Addition of oxidized ubiquinone-10 after sample resuspension restores the original extent of the slow phase (>90%), even in the driest samples (see Fig. 1 *C*, trace *c″*, and Table 1, samples *c* and *d*). This shows that the partial irreversibility of the effects induced by prolonged dehydration of the trehalose samples is not due to irreversible damages of the Q_B site.

Interestingly, partial reduction of redox centers induced by drying has been recently observed by electron paramagnetic

resonance in membrane fragments from a photosynthetic bacterium (Lieutaud et al., 2003).

The above points indicate that, when trivial effects due to the prereduction of Q_B in a fraction of RCs are taken into account, dehydration of the trehalose matrix reversibly impairs electron transfer to Q_B at room temperature.

Fig. 2 summarizes the results of the kinetic analysis of P^+ decay performed in trehalose solutions and in a series of dehydrated amorphous matrices. Kinetic parameters, obtained from traces similar to those shown in Fig. 1, are plotted as a function of trehalose concentration. In Fig. 1 *A*, the amplitude of the slow component of P^+ decay measured in dehydrated amorphous samples (trehalose concentration ≥90 wt %) has been normalized to that determined upon resuspension of the same matrix. This procedure corrects for the extent of the fast P^+ recombination due to prereduction of Q_B (see above) and allows an estimate of the fraction of RC in which Q_A^--to-Q_B electron transfer is reversibly inhibited. The amplitudes measured in the liquid samples have been normalized to that measured at 16 wt % (i.e., at the trehalose concentration obtained upon resuspension of dehydrated samples). Fig. 2 corroborates and better defines the behavior indicated by the data of Fig. 1 and Table 1. The increase of trehalose concentration above 90 wt % results in the appearance of a fast rate distribution. The amplitude of this kinetic component increases with dehydration and predominantly accounts for P^+ decay at ~97 wt % trehalose (Fig. 2 *A*). The values measured for the average rate constant, $\langle k_f \rangle$, and for the width, σ_f, of this fast rate distribution (Fig. 2 *B*) are quantitatively consistent with those measured for $P^+Q_A^-$ recombination at the corresponding trehalose concentrations in RC deprived of Q_B (Palazzo et al., 2002). The residual slow kinetic component ($P^+Q_B^-$ recombination) exhibits an average rate constant ($\langle k_s \rangle$) which decreases when the trehalose concentration increases up to ~90 wt % (Fig. 2 *C*). Under these conditions, Q_A^--to-Q_B electron transfer remains fast compared to the recombination of $P^+Q_A^-$ (i.e., $k_{AB} + k_{BA} \gg k_{AP}$) (see below). Since the states $Q_A^-Q_B$ and $Q_AQ_B^-$ are in rapid equilibrium, the observed decrease in the $P^+Q_B^-$ recombination rate seems to reflect a slight stabilization of the charge-separated $P^+Q_B^-$ state with respect to $P^+Q_A^-$. The width σ_s of the slow rate distribution tends to increase with trehalose concentration (Fig. 2 *C*). This slight broadening of the rate distribution likely reflects the decreased interconversion between protein conformational substates with increasing rigidity of the matrix.

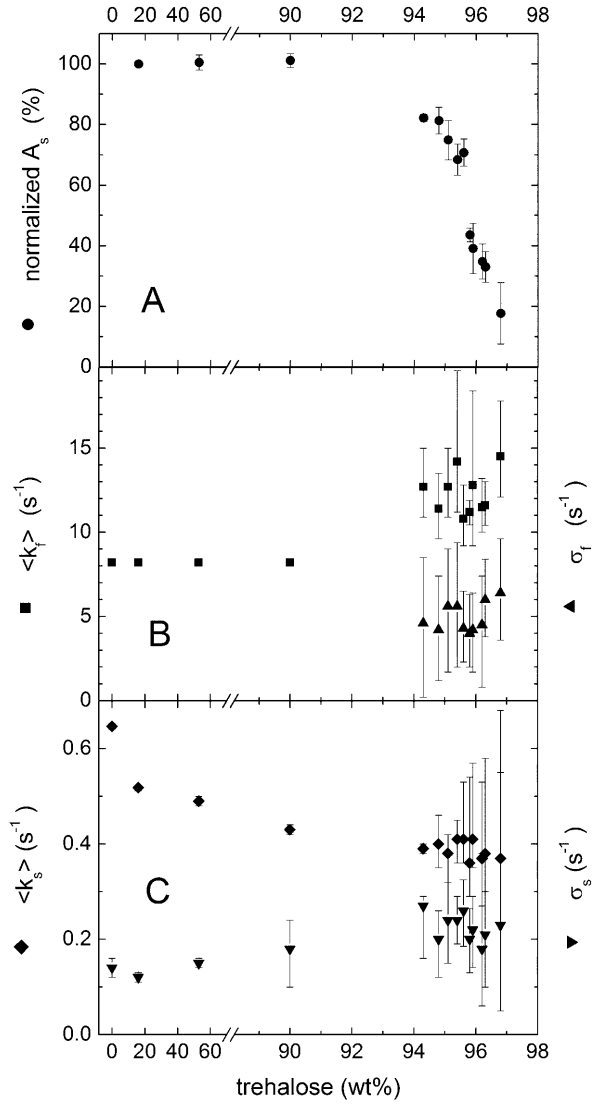

FIGURE 2 Kinetic parameters of charge recombination as a function of trehalose concentration in solution and dehydrated amorphous samples. (*A*) Normalized amplitude A_S of the slow kinetic component (*circles*). (*B*) Average rate constant $\langle k_f \rangle$ (*squares*) and width σ_f (*triangles*) of the fast kinetic component. At trehalose concentrations ≤ 90 wt % the fast kinetic component was fitted to a simple exponential (see Eq. 2) with k_f fixed to 8.2 s^{-1}. Correspondingly, no error bar is associated to $\langle k_f \rangle$ and no σ_f value is plotted at these concentrations. (*C*) Average rate constant $\langle k_s \rangle$ (*diamonds*) and width σ_s (*inverted triangles*) of the slow rate distribution. Error bars give the confidence intervals within two standard deviations. See text for details.

In summary, the effects observed in P^+ recombination kinetics concur in suggesting that progressive dehydration of the trehalose matrix blocks electron transfer to Q_B in an increasing fraction of the RC population. In previous work we showed that extensive dehydration of trehalose-coated RCs (corresponding to trehalose concentrations >97 wt %) is needed for hindering the protein internal motions coupled to $P^+Q_A^-$ charge recombination (Palazzo et al., 2002). By contrast, the present results suggest that a dehydration of trehalose samples resulting in a trehalose concentration increase from 90 wt % to 97 wt % is sufficient for strongly reducing the RC conformational dynamics that gates the Q_A^--to-Q_B electron transfer over the whole RC population. In what follows, we describe complementary experiments aimed at clarifying the modalities of inhibition of Q_A^--to-Q_B electron transfer induced by dehydration.

Comparison with low temperature data: homogeneous vs. heterogeneous inhibition of Q_A^--to-Q_B electron transfer in dehydrated trehalose matrices

When RCs are frozen in the dark, the yield of electron transfer from Q_A^- to Q_B diminishes with temperature, so that almost no reaction is seen at <200 K (Kleinfeld et al., 1984a; Xu and Gunner, 2001). By examining the fraction A_f of fast P^+ decay after a flash, Xu and Gunner (2001) determined the temperature-dependence of the quantum efficiency of $P^+Q_B^-$ formation, defined as $\phi = (1 - A_f) \approx k_{AB}/(k_{AB} + k_{AP})$ (see Eq. 1); they obtained evidence that the decrease of ϕ at low temperatures reflects the competition within a homogeneous RC population between electron transfer from Q_A^- to Q_B (governed by the temperature-dependent rate constant, k_{AB}) and the return to the ground state of $P^+Q_A^-$ (determined by k_{AP}, assumed to be temperature-independent; see Eq. 1). Our data (Fig. 2 *A*) show that for trehalose-coated RCs the fraction A_s of slow P^+ decay after a flash at room temperature decreases in parallel with dehydration of the matrix, practically vanishing in relatively dried matrices. This decrease of A_s upon dehydration resembles the decrease observed at cryogenic temperatures (Xu and Gunner, 2001). However, as mentioned in the previous paragraph, we interpret the decreased extent of $P^+Q_B^-$ recombination in dry samples as due to a block of electron transfer from Q_A^- to Q_B in a fraction of the RC population. Different observations, discussed in the following, suggest in fact that progressive dehydration of the trehalose matrix at room temperature does not slow progressively Q_A^--to-Q_B electron transfer homogeneously over the whole RC population, but rather prevents electron transfer in a progressively increasing subpopulation of the RCs, at least over the timescale of $P^+Q_A^-$ recombination. The increasing fraction of inhibited proteins in turn results in a progressively higher contribution of fast $P^+Q_A^-$ recombination to P^+ decay.

This interpretation is supported by the outcome of a double flash experiment, similar to the one performed at low temperature by Xu and Gunner (2001). The experiment consists in photoexciting the RC sample with two closely spaced flashes, the second flash being fired when most of the $P^+Q_A^-$ RCs have returned to the ground state but the $P^+Q_B^-$ RCs have not. Information is obtained by comparing the kinetics of P^+ decay after the second flash with that observed after a single photoexcitation in the dark-adapted sample. If the fast component of P^+ decay is due to a complete inhibition of the Q_A^--to-Q_B electron transfer in a given subpopulation of RCs, the decay kinetics after the second flash will coincide with the one observed after the first flash. In this case, in fact, the second flash will re-excite the fraction of $P^+Q_A^-$ which has decayed in the time elapsed between the two flashes, thus restoring the situation produced by the first flash. As a consequence, the amplitude and the kinetics of fast phase decay will be the same as after the first flash. On the other hand, if the fast decay results from a decreased quantum yield ϕ of $P^+Q_B^-$, a fraction ϕ of the $P^+Q_A^-$ reformed by the second flash will transfer the electron from Q_A^- to Q_B, thus increasing the slow decaying ($P^+Q_B^-$) fraction. In such a case a lower fast phase amplitude will be observed after the second flash.

Measurements have been performed in a dehydrated trehalose matrix characterized by ~50% fast P^+ decay after a laser flash (Fig. 3). The energy of the laser pulse was increased to reach saturation of P photo-oxidation (as can be seen from the equal amplitude of P^+ absorbance changes induced by the first and second photoexcitations in Fig. 3). The second flash was fired 380 ms after the first photoexcitation, i.e., when the fast phase of P^+ decay after the first flash had essentially decayed. As shown in Fig. 3 (*inset*), the decay after the second flash overlaps with the one observed after the first flash, indicating that the fast decaying fraction does not decrease after the second photoexcitation. This coincidence was confirmed by fitting to Eq. 4 the recombination kinetics after the second flash and P^+ decay after a single laser pulse recorded in the same dark-adapted sample. The relative amplitude of the fast phase was 46.4% and 45.9% after a single flash and after the second flash, respectively. Analogous results were obtained in similar measurements, in which the dark time between the two photoexcitations was reduced to 280 ms or increased up to 600 ms (not shown). These results clearly show that, at variance with that observed at low temperature by Xu and Gunner (2001), dehydration of the glassy matrix inhibits the Q_A^--to-Q_B electron transfer inhomogeneously.

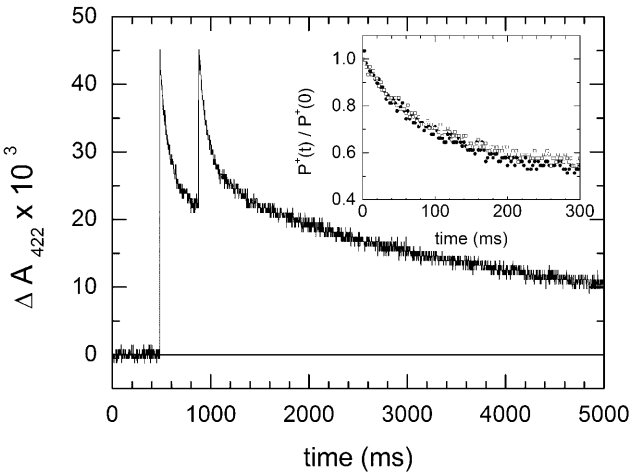

FIGURE 3 Charge recombination kinetics after photo-oxidation of the primary donor *P* induced by two consecutive laser pulses fired 380-ms apart. The trace is the result of a single measurement (without averaging) in a dehydrated trehalose glass. In the inset the normalized P^+ decay after the second (*open squares*) and the first (*solid circles*) laser pulse are superimposed.

An additional argument favoring this view is provided by the kinetic analysis of Eq. 1. As discussed in the Appendix, the inhibition pattern emerging from Fig. 2 appears to be inconsistent with a homogeneous inhibition of Q_A^--to-Q_B electron transfer, as modeled on the basis of the analytical solution of Eq. 1.

The time-resolved electrochromic measurements described below are also consistent with the inhomogeneous character of electron transfer inhibition induced by dehydration.

Kinetics of electrochromic effects associated with Q_A^--to-Q_B electron transfer in trehalose solutions and solid matrices

Electrochromic effects induced in bacteriopheophytin and bacteriochlorophyll bands by the formation of Q_A^- and Q_B^- offer a valuable means to monitor electric charge displacements resulting from Q_A^--to-Q_B electron transfer (Vermeglio and Clayton, 1977; Shopes and Wraight, 1985; Tiede et al., 1996). NIR electrochromism of RC co-factors has revealed complex time- and wavelength-dependent responses to Q_A^--to-Q_B electron transfer in which the contribution of electron transfer and of relaxation processes, such as proton transfer or protein rearrangements, is not easily separated (Tiede et al., 1996, 1998; Li et al., 1998). Recent time-resolved measurements indicate that the kinetics of Q_A^--to-Q_B electron transfer includes at least two kinetic components (Tiede et al., 1996; Li et al., 1998, 2000). With the aim of gaining additional, independent information on the kinetics of Q_A^--to-Q_B electron transfer in trehalose solutions and solid matrices, we measured laser-induced electrochromic absorbance changes at 750 nm. Electrochromic transients recorded in solution and in two dehydrated trehalose matrices have been analyzed in terms of two exponential components. Results are summarized in Table 2. In the absence of trehalose, the lifetimes obtained for the fast and slow phase are respectively ~20 μs and ~160 μs, each component accounting for ~50% amplitude of the kinetics. Considering the large uncertainty resulting from our confidence analysis of fitting (see Materials and Methods), these values compare well with the results of analogous measurements performed in solution at 757 nm (Tiede et al., 1996) and 398 nm (Li et al., 1998). In a 53 wt % trehalose solution, a sizable slowing of both kinetic components is observed; such an effect becomes progressively more pronounced when an amorphous trehalose matrix is formed upon dehydration (Table 2). At 95.4 wt % trehalose, the lifetimes of the fast and slow components increase to ~160 μs and 2.4 ms, respectively. Further drying of the sample prevents a quantitative analysis of the kinetics recorded in the 750-nm region. This is due to a net decrease of the signal amplitude (see traces in Supplemental Material), with the consequent progressive decrease of the signal-to-noise ratio, and to a progressive red shift of the isosbestic point for $P^+Q_A^-$ spectral contributions (see Supplemental Material), which, from ~750-nm, shifts to ~756 nm in the driest samples. This notwithstanding, traces recorded in extensively dehydrated samples (not shown) indicate that: 1), the amplitude of electrochromic signals in plasticized samples decreases upon decreasing the water content and practically vanishes at a trehalose concentration close to 97 wt %; 2), in the driest matrices in which a residual electrochromic signal is detectable, it reaches the maximal amplitude within 5–8 ms from the laser pulse; and 3), upon rehydration a large fraction of the original electrochromic signal and the lifetimes of the two kinetic components measured in solution are essentially restored.

TABLE 2 Parameters of a biexponential fit to the kinetics of electrochromic effects associated with Q_A^--to-Q_B electron transfer

Trehalose concentration (wt %)	A_f (%)	τ_f (μs)	τ_s (μs)
0.0	41 (26,60)	23 (8,45)	159 (115,230)
53.0	60 (44,76)	63 (43,84)	332 (231,592)
90.0	54 (32,72)	92 (46,152)	720 (432,8000)
95.4	59 (35,80)	160 (102,230)	2400 (1800,8500)

A_f, τ_f, and τ_s indicate the fast phase amplitude and the fast and slow lifetimes, respectively. The absorbance change induced by a laser pulse has been measured at 750 nm in liquid samples and trehalose amorphous matrices (samples *a* and *c* of Fig. 1 *B* and Table 1). Values in parentheses give the extremes of the confidence intervals within two standard deviations (see Materials and Methods).

In summary, measurements of the electrochromic response indicate that at trehalose concentrations <~90 wt %, electron transfer to Q_B occurs in essentially all RCs. Both kinetic phases of this process are slowed down with increasing trehalose concentration, suggesting that protein dynamics coupled to Q_A^--to-Q_B electron transfer is moderately slowed down, likely as a result of the increasing viscosity of the external matrix. Under these conditions, Q_A^--to-Q_B electron transfer is still fast enough to compete efficiently with $P^+Q_A^-$ recombination. Accordingly, charge recombination occurs essentially from the $P^+Q_B^-$ state with an average rate constant $\langle k_s \rangle \cong 0.4\ s^{-1}$, lower than in solution (see Fig. 2). Upon increasing the trehalose concentrations above 90 wt %, in amorphous matrices, the extent of the electrochromic signal decreases, suggesting that in a progressively increasing fraction of the RCs population the electron is unable to reach Q_B. This is consistent with the increase observed in the fraction of fast P^+ decay ($P^+Q_A^-$ recombination; Fig. 2 *A*). In the residual RC fraction, as indicated by the kinetics of the residual electrochromic signals, electron transfer to Q_B still successfully competes with $P^+Q_A^-$ recombination. Correspondingly, in these more dehydrated samples the kinetics of the residual slow component of charge recombination ($P^+Q_B^-$) is not further affected ($\langle k_s \rangle \cong 0.4\ s^{-1}$; see Fig. 2 *C*).

Charge recombination after continuous illumination of RCs in dehydrated trehalose matrices

The results presented above strongly suggest that reducing the water content of the trehalose matrix below a critical level inhibits the conformational changes gating the Q_A^--to-Q_B electron transfer, which are likely triggered by the formation of the primary charge-separated state $P^+Q_A^-$. As a result, progressive dehydration of the matrix impairs the Q_A^--to-Q_B electron transfer in an increasing fraction of RCs. To evaluate to which extent the transition from the inactive to the active conformation is slowed down in this inhibited RC population, we studied the kinetics of charge recombination after continuous illumination of the sample (from a few ms to seconds). The underlying idea is that continuous illumination, keeping the RC in the primary charge-separated state ($P^+Q_A^-$) for a sufficiently long time, will eventually allow the slowed conformational transition to occur in the ''inhibited'' fraction of the RCs. In this case, we expect that the kinetics of P^+ decay, after a sufficiently long and intense photoexcitation, will show a larger fraction of the slow phase, as compared to the kinetics monitored after a short laser pulse.

The results of such measurements, performed in three samples labeled 1, 2, and 3, characterized by an increased dehydration and exhibiting an increasing inhibition of Q_A^--to-Q_B electron transfer, are shown in Fig. 4. Fig. 4 *A* compares kinetic traces of charge recombination measured in a moderately dehydrated sample (sample 2 in Fig. 4 *B*) after a laser pulse (trace *a*), a 300-ms (trace *b*), and a 3.5-s (trace *c*) period of continuous illumination. In this sample, the amplitude of the residual slow phase of P^+ decay, 57% of the total when the RC is photoexcited by a laser pulse, increases to 67% and 76% after continuous photoexcitations of 300 ms and 3.5 s, respectively. Under all tested conditions (different dehydration of the sample, different duration of photoexcitation) P^+ decay could be accurately fitted to the sum of two power laws (Eq. 4). The relative amplitude of the slow kinetic component obtained in samples 1–3 is plotted in Fig. 4 *B*, as a function of the duration of photoexcitation. The other kinetic parameters of P^+ decay (not shown) do not exhibit any dependence upon the period of continuous illumination: the values of $\langle k_f \rangle$ range between 9 s^{-1} and 13 s^{-1}, increasing from sample 1 to sample 3; the corresponding values of $\langle k_s \rangle$, σ_s, and σ_f fluctuate at ~0.4 s^{-1}, 0.2 s^{-1}, and 5 s^{-1}, respectively, in agreement with fitting of P^+ decay after a laser pulse (see Fig. 2).

As expected, the relative amplitude of the slow kinetic component (Fig. 4 *B*) systematically increases with the duration of illumination, showing that, when the charge-separated state is maintained for a sufficiently long time, electrons can reach the secondary acceptor Q_B also in RCs that are part of the ''inhibited'' population. A control experiment performed in solution (not shown) demonstrated

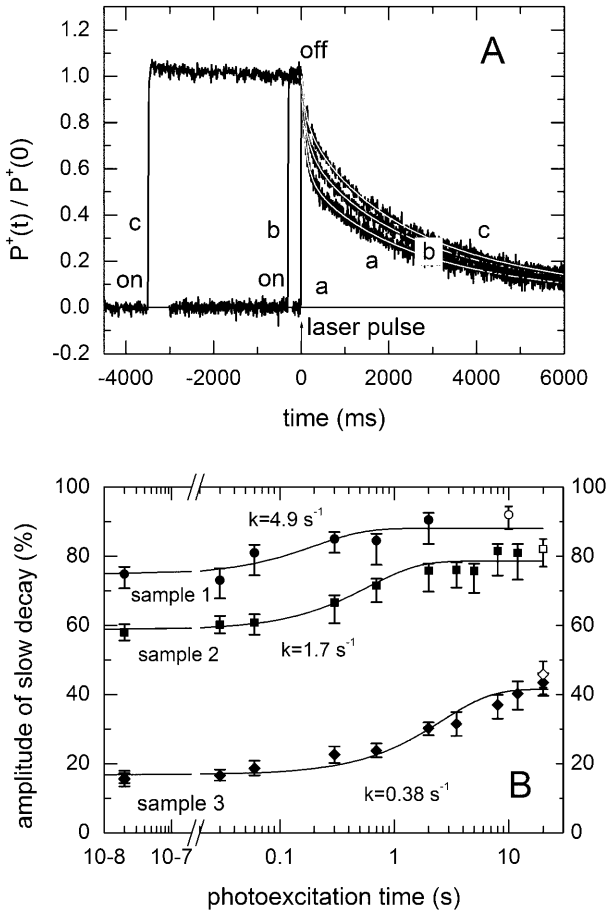

FIGURE 4 Kinetics of charge recombination after continuous illumination of RCs embedded in dehydrated trehalose matrices. (*A*) Normalized P^+ decay after a laser pulse (trace *a*) and continuous illumination of 300 ms (trace *b*) and 3.5 s (trace *c*) duration in a moderately dehydrated matrix (sample 2 in *B*). Continuous curves are best fit to the sum of two power laws (Eq. 4). (*B*) Amplitude of the slow component of charge recombination as a function of the duration of photoexcitation at increasing degree of dehydration of the trehalose matrix. Data were obtained by fitting P^+ decay to Eq. 4 as shown in *A*. The trehalose concentration was 94.8 wt %, 95.6 wt %, and 96.3 wt % in samples 1, 2, and 3, respectively. Continuous curves represent best fit to exponential kinetics characterized by rate constants of 4.9 s^{-1}, 1.7 s^{-1}, and 0.38 s^{-1}, for samples 1, 2, and 3, respectively.

that after continuous illumination up to 20 s (i.e., the longer excitation time used in trehalose matrices), charge recombination exhibits kinetics independent of the duration of illumination and coincident with those measured after a 20-ns laser pulse. The effects reported in Fig. 4 are observed only when RCs are embedded in plasticized amorphous matrices and are not, therefore, intrinsic properties of RC. Interestingly, as shown in Fig. 4 *B*, the recovery kinetics of the slow phase amplitude at increasing photoexcitation time are much faster in the ''wet'' sample than in more dried matrices. Exponential fitting gives k = 4.9 s^{-1}, 1.7 s^{-1}, and 0.38 s^{-1}, in samples 1, 2, and 3, respectively. Moreover, for each sample, the maximal amplitude of the slow phase reached after continuous

illumination is very close to that observed when samples are redissolved (Fig. 4 *B*, *open symbols*). This indicates that, except for RCs having chemically prereduced Q_B (see above), the other reaction centers can catalyze Q_A^--to-Q_B electron transfer after suitably long continuous illumination.

We conclude that the recovery kinetics of the slow phase of charge recombination after a period of continuous illumination reflect the kinetics of the conformational change(s) gating Q_A^--to-Q_B electron transfer in the inhibited population of RCs. The transition, indeed, does not occur in this fraction of RCs when a short laser pulse excites *P*, since it would be too slow to compete successfully with $P^+Q_A^-$ recombination. Consistently, the rate constant that characterizes the recovery kinetics of the slow component of charge recombination (Fig. 4 *B*), is always smaller than that (k_{AP}) of $P^+Q_A^-$ recombination (from a factor 2 in ''wet'' sample 1, to almost two orders of magnitude in sample 3). After continuous illumination of increasing duration, the transition from the inactive to the active conformation can be monitored: its kinetics are markedly slowed down upon dehydration, likely due to the hardening of the glassy matrix. By comparing the recovery kinetics of the amplitude of the slow recombination component shown in Fig. 4 *B* with the kinetics measured for Q_A^--to-Q_B electron transfer in solution, exploiting the electrochromic effects, one can estimate the extent to which the incorporation into dehydrated matrices slows down the transition from the inactive to the active conformation. Even assuming that only the slow phase of the electrochromic effects associated with Q_A^--to-Q_B electron transfer reflects the gating conformational change, it appears that in the more extensively dehydrated trehalose matrix the transition from the inactive to the active conformation is slowed by at least four orders of magnitude. In fact, it can be evaluated that the rate constant *k* of the gating conformational change decreases from $\sim 6 \times 10^3\ s^{-1}$ in solution ($\tau_s \approx 160\ \mu s$, in the absence of trehalose; see Table 2) to $3.8 \times 10^{-1}\ s^{-1}$ (Fig. 4 *B*, sample 3).

Effects of dehydration and role of trehalose

To better understand the role of trehalose in the effects described above and to examine to what extent dehydration per se inhibits Q_A^--to-Q_B electron transfer, we studied the kinetics of P^+ decay in dehydrated RC films, in the absence of the sugar. As already observed with RCs deprived of Q_B (Palazzo et al., 2002), in the absence of trehalose, a few hours of exposure to a flow of dry N_2 causes exhaustive sample dehydration. Indeed, no absorption is detected in the NIR band at 1950 nm, which we exploited for estimating the sample water content (Fig. 5 *B*, *lower spectrum*). Kinetic analysis of P^+ decay (Fig. 5 *A*, trace *a*) shows that, under these conditions, in ~50% of the RC population fast recombination occurs from the $P^+Q_A^-$ state. Resuspension of the film results in a considerable recovery of the slow phase amplitude ($A_s = 0.8$, not shown), which is essentially complete upon addition of ubiquinone-10 (Fig. 5 *A*, trace *b*). In the absence of trehalose, therefore, dehydration reversibly inhibits Q_A^--to-Q_B electron transfer in a fraction of the RC population. However, the behavior observed in trehalose matrices is substantially different. Upon dehydration, a comparable inhibition of Q_A^--to-Q_B electron transfer,

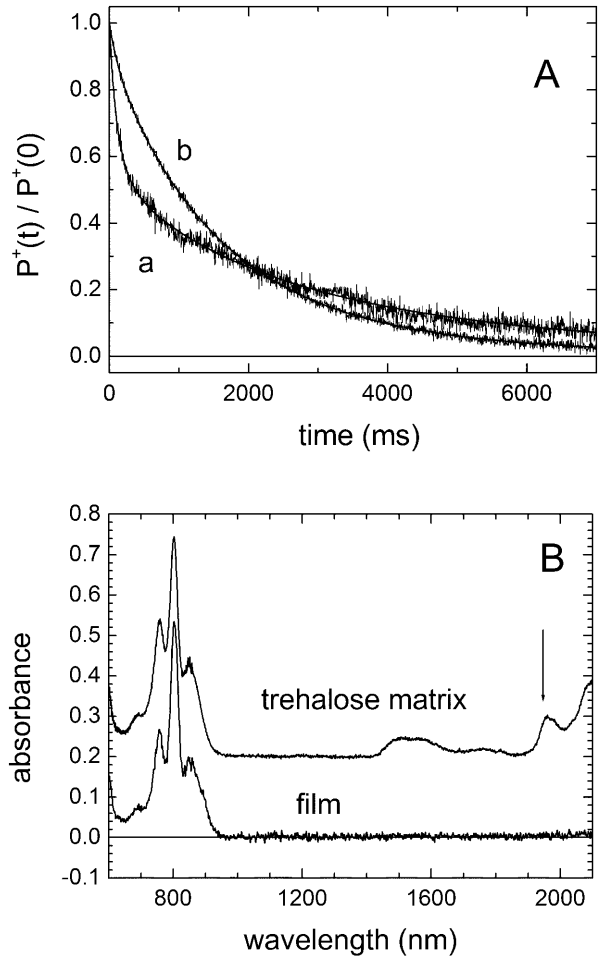

FIGURE 5 Kinetics of charge recombination in RC dried without trehalose. (*A*) Normalized P^+ decay in a dry film (trace *a*) and after resuspension of the film and addition of 60 μM ubiquinone-10 in LDAO (final detergent concentration 0.06%; trace *b*). The *solid line* through trace *a* is a fit to Eq. 4, yielding the following values of parameters according to Eq. 5: $A_s = 0.49$ (0.46, 0.51); $\langle k_s \rangle = 0.42\ s^{-1}$ (0.37, 0.43); $\sigma_s = 0.22\ s^{-1}$ (0.18, 0.25); $\langle k_f \rangle = 8.7\ s^{-1}$ (7.6, 10.4); and $\sigma_f = 2.3\ s^{-1}$ (0, 5.1). Continuous curve through trace *b* represents a fit according to Eq. 2 with k_f fixed to $8.2\ s^{-1}$; best fitting yields $A_f = 0.097$ (0.085, 0.108); $\langle k_s \rangle = 0.628\ s^{-1}$ (0.624, 636); and $\sigma_s = 0.19\ s^{-1}$ (0.18, 0.20). Values in parentheses indicate the extremes of the confidence intervals of the fitting parameters within two standard deviations. (*B*) The visible NIR spectrum recorded in the dry RC film (*lower spectrum*) is compared to the spectrum recorded in a dehydrated trehalose matrix (95.4 wt % trehalose). The kinetics of charge recombination recorded in this sample is shown in Fig. 1 *B* as trace *c*. The position of the water combination band at 1950 nm is indicated by the arrow. The two spectra have been normalized at the maximal amplitude at 802 nm and the spectrum of the trehalose matrix has been offset by 0.2 absorbance units for the sake of visual clarity.

resulting in ~50% fast P^+ recombination, occurs in the saccharide glass at a higher water content (see Fig. 5 *B*, *upper spectrum*) as compared to the RC dried in the absence of trehalose. Actually an almost complete inhibition of the reaction (see Fig. 2 *A*) is observed in trehalose samples at ~97 wt % trehalose, corresponding to $>10^4$ water molecules per RC. By contrast, if RC films are dehydrated in the absence of trehalose, inhibition of Q_A^--to-Q_B electron transfer can be achieved only in a limited fraction of the RC population, despite extremely low water contents. Although extensive dehydration per se affects markedly the yield of Q_B^- formation, a much more effective inhibition of conformational dynamics assisting Q_A^--to-Q_B electron transfer occurs in moderately dehydrated trehalose-coated RCs as compared to RCs dried in the absence of trehalose. Analogous evidences of a specific role of the trehalose matrix in affecting the protein dynamics were obtained when studying $P^+Q_A^-$ recombination in RCs deprived of the secondary quinone acceptor (Palazzo et al., 2002). In this system extensive RC dehydration in the absence of the saccharide had almost no effect on $P^+Q_A^-$ recombination kinetics, which exhibited a very narrow rate distribution ($\sigma \cong 5\ s^{-1}$) centered at $\langle k \rangle \cong 11\ s^{-1}$, a value close to the one measured in solution. In agreement with this observation, in dry films of RCs in the presence of the secondary acceptor Q_B, the fast phase of P^+ decay was characterized by a narrow spectrum of rate constants ($\sigma_f = 2.3\ s^{-1}$) centered at $\langle k_f \rangle = 8.7\ s^{-1}$ (Fig. 5 *A*, fit to trace *a*). These results suggest that in the absence of trehalose, at a very low water content, the RC protein retains some conformational flexibility; interestingly (see below), under such conditions, whereas $P^+Q_A^-$ recombination kinetics is scarcely affected, electron transfer to Q_B is hampered reversibly in almost half of the RC population.

The larger inhibition of the conformational dynamics associated with Q_A^--to-Q_B electron transfer in our RC/water/trehalose system can be rationalized on the basis of recent findings (Cottone et al., 2001, 2002). The authors reported that in a trehalose-water-myoglobin system (89% w/w trehalose concentration), structures are formed containing trehalose molecules, mainly bound to the protein through single hydrogen bonds, and water molecules in excess over their concentration in the bulk solvent. In such structures the myoglobin molecule is confined within a network of hydrogen bonds connecting protein groups, water molecules, and trehalose molecules. Moreover, the fraction of water molecules forming multiple hydrogen bonds with both protein and sugar increased as the water content was lowered. Since increasing the number of hydrogen bonds in which each molecule is involved decreases the motional freedom of the water, one can infer that the hindering of the protein conformational dynamics in trehalose-coated systems is driven by the decreasing water molecules mobility, when the trehalose concentration is increased.

The relationship between conformational relaxation of the $P^+Q_A^-$ state and electron transfer to Q_B

The kinetic analysis of charge recombination in trehalose samples enables one to monitor at the same time the effect of dehydration on two electron transfer processes. The average rate constant $\langle k_f \rangle$ and the distribution width σ_f of the fast component of P^+ decay give information on the distributed kinetics of recombination between P^+ and Q_A^-. The kinetics of this process has been considered as a probe of RC internal dynamics (Kleinfeld et al., 1984a; Feher et al., 1987; McMahon et al., 1998; Palazzo et al., 2002). On the other hand, the relative amplitude of the slow phase of P^+ decay (A_s) measures the fraction of the RC population in which Q_A^--to-Q_B electron transfer occurs at a rate high enough to compete successfully with $P^+Q_A^-$ recombination. The relationship between these two parameters, obtained from the data of Fig. 2, *A* and *B*, is presented in Fig. 6. When Q_A^--to-Q_B electron transfer is inhibited in a increasing fraction of RCs, i.e., A_s decreases, the average rate of $P^+Q_A^-$ recombination, $\langle k_f \rangle$, never exceeds values of 12–14 s^{-1}, even at an almost complete inhibition of Q_A^--to-Q_B electron transfer. The corresponding values of the rate distribution width, σ_f, obtained in these matrices range between 4 s^{-1} and 6 s^{-1} (see Fig. 2 *B*).

When Q_B-deprived RCs are embedded in extensively dehydrated trehalose matrices (trehalose concentration > 97 wt %), the structural changes associated with primary charge separation are completely blocked on the timescale of $P^+Q_A^-$ recombination (Palazzo et al., 2002). Such a block results in an increase of the average rate constant ($\langle k_f \rangle$) of $P^+Q_A^-$ recombination from ~9 s^{-1} to 27 s^{-1} (Palazzo et al., 2002) (see *arrows* in Fig. 6). Correspondingly, thermal fluctuations between conformational substates are frozen, thus broadening the rate distributions (σ increases from ~2 s^{-1} in solution up to 17 s^{-1}). Analogous results were obtained when these dynamics were blocked by lowering the temperature to <80 K (McMahon et al., 1998). As shown in Fig. 6, the $\langle k_f \rangle$ values measured at trehalose concentration that block Q_A^--to-Q_B electron transfer are close to those measured in liquid RC solutions. This suggests that the conformational dynamics and the RC relaxation probed by $P^+Q_A^-$ recombination are very poorly reduced under conditions in which, on the contrary, the conformational change that promotes Q_A^--to-Q_B electron transfer is blocked in the majority of the RC population. Also, in the dried RC film in the absence of trehalose (Fig. 6, *open symbol*), a considerable (40%) reversible inhibition of electron transfer to Q_B was associated with $\langle k_f \rangle = 8.7\ s^{-1}$ and $\sigma_f = 2.3\ s^{-1}$. These observations suggest that the conformational changes that gate Q_A^--to-Q_B electron transfer, although triggered by $P^+Q_A^-$ charge separation, do not simply coincide with the relaxation processes that stabilize the primary charge-separated state, but involve further rearrangements of the RC-solvent system.

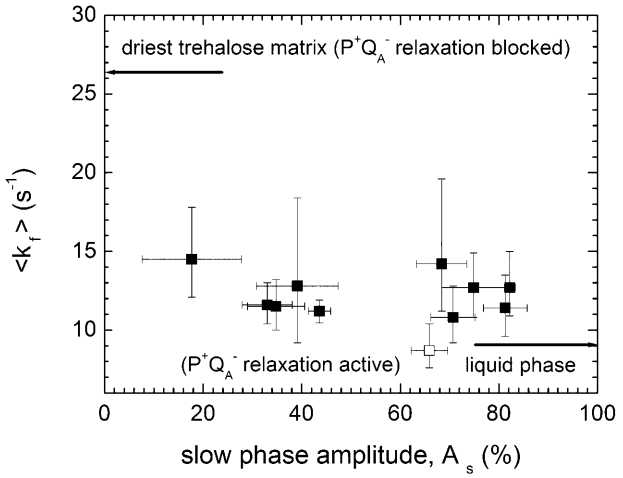

FIGURE 6 Average rate constant of the fast phase of charge recombination ($\langle k_f \rangle$) as a function of the corresponding amplitude of the slow kinetic component (A_s) in a series of trehalose samples (see Fig. 2, *A* and *B*) characterized by a different degree of dehydration (*solid squares*) and in a dehydrated RC film in the absence of trehalose (*open square*). The relative amplitude A_s is normalized to the amplitude of the slow phase determined upon resuspension of the dehydrated matrix. The arrows pointing to the right and to the left indicate the average rate constant of $P^+Q_A^-$ recombination measured in the absence of Q_B in solution, and in a solid trehalose matrix, extensively dehydrated, respectively (Palazzo et al., 2002). Error bars give the confidence intervals within two standard deviations.

A variety of structural changes have been proposed as responsible for the gating of electron transfer to Q_B. The accumulated x-ray data show several positions and orientations for Q_B, which can be brought back essentially to two possible binding sites (Walden and Wheeler, 2002). In the crystal structure of the RC cooled to cryogenic temperatures under illumination, i.e., trapped in an active state, Q_B was found 2.7 Å closer to Q_A than in the protein frozen in the dark and flipped by 180° around the isoprenoid chain (Stowell et al., 1997). The movement of Q_B from an inactive-distal to an active-proximal site was proposed as the major structural change involved in the conformational gating step (Stowell et al., 1997). However, a mutated RC (L209PY), in which Q_B was found in the crystal structure in the proximal position even in the dark (Kuglstatter et al., 2001), exhibited practically the same rate of Q_A^--to-Q_B electron transfer as the wild-type (Baciou and Michel, 1995). Moreover, a temperature-dependence study in L209PY RCs reveals a behavior quite similar to that observed in wild-type RCs, indicating that a considerable barrier to $Q_A^- \rightarrow Q_B$ electron transfer is still present when Q_B is in the proximal position (Xu et al., 2002). Actually an analysis of light-induced FTIR absorption changes associated with the reduction of Q_B favors a unique binding site at the proximal position both in wild-type and in L209PY RCs (Breton et al., 2002). The movement of Q_B does not seem, therefore, to represent the dominant contribution to the conformational gate that controls electron transfer to Q_B. Internal proton shifts, dielectric responses of the protein residues, and changes in the hydrogen bonding pattern have been alternatively proposed to play a role in the gating mechanism and possibly cooperate in determining a quite complex energy landscape associated with the electron transfer to Q_B (Xu and Gunner, 2001; 2002; Xu et al., 2002). In line with this view, our results show that the gating processes are inhibited at room temperature in moderately dehydrated trehalose matrices, in which the kinetics of $P^+Q_A^-$ recombination, i.e., an electron transfer reaction spanning the RC hydrophobic core, is scarcely affected.

CONCLUSIONS

The electron transfer reaction $Q_A^-Q_B \rightarrow Q_AQ_B^-$ has been proposed to be rate-limited by conformational gating (Graige et al., 1998); this conclusion was reached mainly on the basis of driving force assay and low-temperature studies. The present article yields independent support to such a reaction mechanism: it shows, in fact, that electron transfer to Q_B is hindered at room temperature in trehalose-coated RCs by a limited decrease of the residual water in the samples.

The reported results allow the following further conclusions:

The reversible block of Q_A^--to-Q_B electron transfer caused by dehydration can be ascribed to a large, inhomogeneous increase of the energy barriers that govern the conformational gate. Indeed, the response to dehydration involves at least two subpopulations of RCs. In one of them, Q_A^--to-Q_B electron transfer is slowed by dehydration, but still competes efficiently with $P^+Q_A^-$ recombination even in the more dried samples. In the other subpopulation electron transfer to Q_B is not observed, being unable to compete with $P^+Q_A^-$ recombination. Residual water modulates the relative fraction of the two subpopulations; the active subpopulation is reduced progressively to zero by dehydration.

The inactive RC subpopulation, incompetent for flash-induced electron transfer to Q_B, can catalyze the reduction of Q_B when excited by continuous, saturating illumination for a sufficiently long time. In this inactive fraction of RCs, the conformational transition to active substates is slowed progressively upon dehydration of the amorphous trehalose matrix (see Fig. 4 *B*). It appears that in extensively dehydrated trehalose matrices the conformational change gating Q_A^--to-Q_B electron transfer is slowed by at least four orders of magnitude as compared to RC in solution.

Dehydration in the absence and in the presence of trehalose has qualitatively similar effects on electron transfer to Q_B, suggesting that water-protein interactions play an important role in the gating process. However, in the absence of trehalose, Q_A^--to-Q_B

electron transfer is blocked only in a fraction (≤50%) of the RC population even under conditions of extreme drought. The quantitatively different dynamic behavior observed in samples dried in the presence of the sugar puts forward the relevance of hydrogen bond networks in blocking protein conformations.

- A comparison of the effects of dehydration on the rate of $P^+Q_A^-\rightarrow PQ_A$ recombination and of $Q_A^-Q_B\rightarrow Q_AQ_B^-$ electron transfer (see Fig. 6) indicates that the protein-solvent relaxation stabilizing $P^+Q_A^-$ is different from the conformational transition(s) that gate(s) electron transfer to Q_B. Indeed, in trehalose solid matrices, both reactions are affected by a small variation of the residual water content, but at different degrees of sample hydration.

The reported results indicate that studying electron transfer kinetics at room temperature as a function of residual water in solid trehalose matrices can successfully complement the information coming from low-temperature measurements.

APPENDIX

The rate equations describing the time-evolution of the RC states in Eq. 1 are

$$\begin{aligned}\frac{dx_1}{dt} &= k_{AP}x_2 + k_{BP}x_3\\ \frac{dx_2}{dt} &= -(k_{AP}+k_{AB})x_2 + k_{BA}x_3\\ \frac{dx_3}{dt} &= k_{AB}x_2 - (k_{BA}+k_{BP})x_3,\end{aligned} \tag{A1}$$

where x_1, x_2, and x_3 represent the fraction of the RC population in the PQ_AQ_B, $P^+Q_A^-Q_B$, and $P^+Q_AQ_B^-$ states, respectively. We assume the initial conditions $x_1(0) = x_3(0) = 0$, $x_2(0) = 1$, i.e., at $t = 0$, after a short saturating flash of light, all reaction centers are in the primary charge-separated state $P^+Q_A^-Q_B$.

The solution of Eq. A1 is:

$$\begin{aligned}x_1(t) &= \left[\frac{k_{AP}(k_{BA}+k_{BP}+r_1)+k_{BP}k_{AB}}{r_1(r_1-r_2)}\right]\exp(r_1t)\\ &\quad+\left[\frac{k_{AP}(k_{BA}+k_{BP}+r_2)+k_{BP}k_{AB}}{r_2(r_2-r_1)}\right]\exp(r_2t)+1\\ x_2(t) &= \frac{k_{BA}+k_{BP}+r_1}{r_1-r_2}\exp(r_1t)+\frac{k_{BA}+k_{BP}+r_2}{r_2-r_1}\exp(r_2t)\\ x_3(t) &= \frac{k_{AB}}{r_1-r_2}\exp(r_1t)+\frac{k_{AB}}{r_2-r_1}\exp(r_2t),\end{aligned} \tag{A2}$$

where the roots of the characteristic equation, r_1 and r_2, are given by

$$r_{1,2} = -\left(\frac{k_{AP}+k_{AB}+k_{BA}+k_{BP}}{2}\right)\pm\left[\left(\frac{k_{AP}+k_{AB}+k_{BA}+k_{BP}}{2}\right)^2-(k_{AP}k_{BA}+k_{AP}k_{BP}+k_{AB}k_{BP})\right]^{1/2}. \tag{A3}$$

The normalized P^+ decay after a flash can be modeled as $P^+(t)/P^+(0) = x_2(t) + x_3(t)$, i.e., according to Eqs. A2 and A3, as the sum of two (fast and slow) decaying exponentials.

To explore the effects of a progressive inhibition of Q_A^--to-Q_B electron transfer on charge recombination kinetics within a homogeneous RC population, we divide k_{AB} and k_{BA} by a factor ≥1 (degree of inhibition) α and β, respectively, in Eqs. A2 and A3. Therefore, the relative amplitude of the fast phase A_f of P^+ decay as a function of α and β will be

$$A_f(\alpha,\beta) = \frac{k_{AB}/\alpha + k_{BA}/\beta + k_{BP} + k_f(\alpha,\beta)}{k_f(\alpha,\beta) - k_s(\alpha,\beta)}, \tag{A4}$$

being the rate constant of the fast $k_f(\alpha, \beta)$ and slow $k_s(\alpha, \beta)$ phase of P^+ decay given by

$$k_{s,f} = -\left(\frac{k_{AP}+k_{AB}/\alpha+k_{BA}/\beta+k_{BP}}{2}\right)\pm\left[\left(\frac{k_{AP}+k_{AB}/\alpha+k_{BA}/\beta+k_{BP}}{2}\right)^2-(k_{AP}k_{BA}/\beta+k_{AP}k_{BP}+k_{AB}k_{BP}/\alpha)\right]^{1/2}, \tag{A5}$$

in which the + and − signs refer to the slow and fast components, respectively.

Fig. A1 (*open circles*) shows plots of $A_f(\alpha)$, $k_f(\alpha)$, and $k_s(\alpha)$ (A, B, and C, respectively), calculated according to Eqs. A4 and A5 under the simplifying assumption that the direct and reverse rate constant are decreased by the same factor ($\alpha = \beta$), i.e., that no change in the equilibrium constant K_{AB} for Q_A^--to-Q_B electron transfer occur in parallel with inhibition. The following representative values have been assumed for the kinetic constants of Eq. 1: $k_{AB} = 6\times10^3\ s^{-1}$ and $k_{BA} = 4.5\times10^2\ s^{-1}$, based on measurements at room temperature at $6.0 < pH < 8.0$ (Kleinfeld et al., 1984b); and $k_{BP} = 0.1\ s^{-1}$ on the basis of values obtained at pH 7.4 and in the 277 K ÷ 313 K temperature interval by Labahn et al. (1995). A value of $k_{AP} = 10\ s^{-1}$ (Kleinfeld et al., 1984b), independent of the degree of inhibition, was also assumed.

The effects of a possible change in K_{AB} as well as in k_{AP} have been estimated on the basis of the experimentally observed response to dehydration of kinetic parameters of P^+ recombination and electrochromic effects. According to Eq. 1, when the direct route (k_{BP}) of $P^+Q_AQ_B^-$ recombination is negligible and the states $P^+Q_AQ_B^-$ and $P^+Q_A^-Q_B$ are in rapid equilibrium on the timescale of $P^+Q_A^-Q_B$ recombination, the equilibrium constant $K_{AB} = (k_{AB}/k_{BA})\ (\beta/\alpha)$ can be expressed as (Kleinfeld et al., 1984b; Mancino et al., 1984):

$$K_{AB} = (k_f - k_s)/k_s. \tag{A6}$$

As shown in Fig. 2 *C*, the average rate constant $\langle k_s\rangle$ of the slow P^+ decay decreases from ~0.7 s^{-1} to a minimum value close to 0.4 s^{-1} when the trehalose concentration increases from 0 to 90 wt %. According to Eq. A6, for $k_f = 10\ s^{-1}$, this behavior would correspond to an increase of K_{AB} from 13.3 to 24.0, when the trehalose concentration is varied from 0 wt % to 90 wt %. Such a change in K_{AB} yields an increase of β/α from 1 to 1.8. Upon increasing trehalose concentration to 90 wt %, both kinetic phases of the electrochromic effects coupled to Q_A^--to-Q_B electron transfer are slowed by a comparable factor of ~4.3 (see Table 2). Therefore, $(k_{AB}/\alpha + k_{BA}/\beta)$ can be assumed to decrease approximately by a factor of 4.3 when the trehalose concentration increases from 0 to 90 wt %. By combining this information, it can be easily evaluated that $\beta/\alpha \approx 1.8$ at $\alpha \approx 4.2$. Upon further increasing the trehalose concentration up to 97 wt %, $\langle k_s\rangle$ remains essentially constant at ~0.4 s^{-1} (Fig. 2 *C*), whereas $\langle k_f\rangle$ increases up to a maximum value of ~14 s^{-1} (Fig. 2 *B*). According to Eq. A6, this would correspond to a maximal increase of K_{AB} to 34, i.e., to $\beta/\alpha \approx 2.6$. To

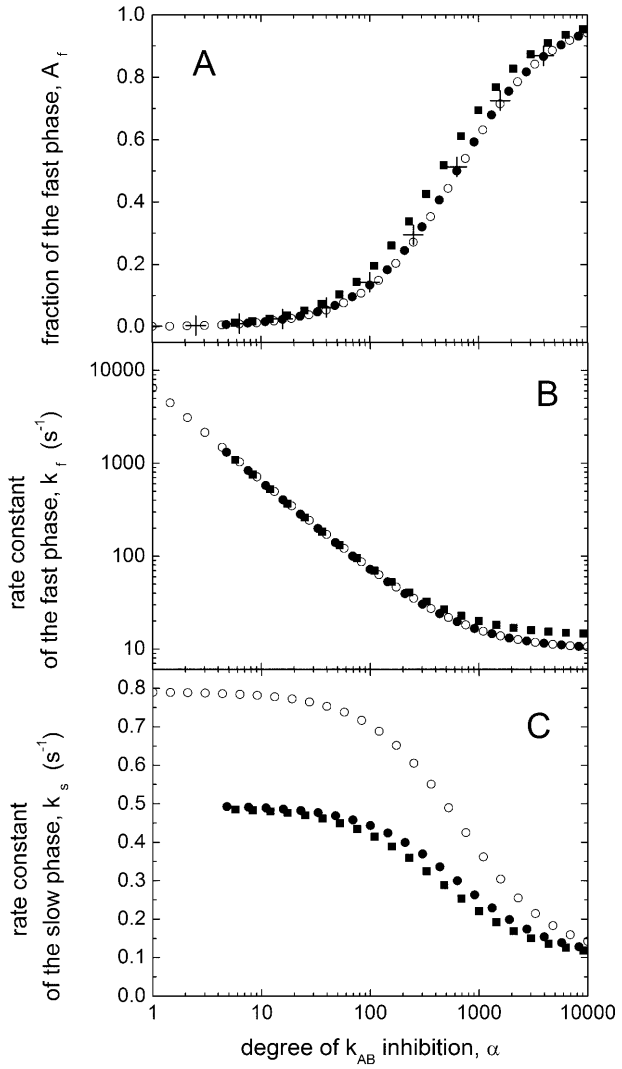

FIGURE A1 Predicted dependencies of the kinetic parameters of charge recombination upon the degree of inhibition, α, of the direct (k_{AB}) electron transfer reaction from Q_A^- to Q_B. The fraction A_f of fast P^+ decay (*A*); the rate constant of the fast, k_f (*B*); and slow, k_s (*C*) kinetic components are calculated according to Eqs. A4 and A5. Numerical values assumed for k_{BP}, k_{AB}, and k_{BA} are given in the Appendix. Different values have been considered for k_{AP} and for the degree of inhibition, β, of the reverse (k_{BA}) electron transfer reaction from Q_B^- to Q_A (see Appendix): $k_{AP} = 10\ s^{-1}$, $\beta = \alpha$ (*open circles*); $k_{AP} = 10\ s^{-1}$, $\beta = 1.8\ \alpha$ (*solid circles*); and $k_{AP} = 14\ s^{-1}$, $\beta = 2.6\ \alpha$ (*solid squares*). In *A*, the A_f values evaluated through the approximation $\phi = 1 - A_f \approx k_{AB}/(k_{AB} + k_{AP})$ are shown as crosses.

evaluate the possible effects of such changes in K_{AB} and k_{AP}, we show in Fig. A1 the inhibition patterns predicted for $\beta/\alpha = 1.8$ and $k_{AP} = 10\ s^{-1}$ (*solid circles*) as well as for $\beta/\alpha = 2.6$ and $k_{AP} = 14\ s^{-1}$ (*solid squares*). In all the conditions considered, the contribution of the direct recombination route (k_{BP}) is practically negligible, since decreasing its value to zero does not affect significantly the behavior emerging from Fig. A1. For the sake of comparison, Fig. A1, *A*, also shows the α-dependence of the fraction of fast phase, A_f, evaluated under the approximation $\phi = 1 - A_f \approx k_{AB}/(k_{AB} + k_{AP})$ (*crosses*). This approximate relation, which well-reproduces the values calculated from Eqs. A4 and A5, under the different assumptions considered, has been extensively used to evaluate k_{AB} from the analysis of charge recombination kinetics (Xu and Gunner, 2001, 2002; Xu et al., 2002).

An inspection of the plots in Fig. A1 shows that the appearance of a fast phase in P^+ decay (≈10%) requires an increase of the degree of inhibition α by more than one order of magnitude (Fig. A1, *A*). When α is further increased by two orders of magnitude, the fast phase almost completely accounts for P^+ decay (≈90%). Over this range of Q_A^--to-Q_B inhibition, however, the rate constant which characterizes the fast phase of P^+ decay is not constant, but decreases by one order of magnitude approaching that of $P^+Q_A^-$ recombination (k_{AP}) only when Q_A^--to-Q_B electron transfer is strongly inhibited, i.e., when the amplitude of the fast phase of P^+ decay is >80% (Fig. A1, *B*). The model predicts a similar inhibition pattern, when considering the changes in K_{AB} and k_{AP} discussed above.

By contrast, in dehydrated trehalose matrices, we find experimentally that the rate constant of the fast phase does not decrease and always reflects that of $P^+Q_A^-$ recombination, independently of the degree of dehydration, i.e., of the corresponding relative amplitude of the fast phase (Fig. 2, *A* and *B*). The change observed experimentally in $\langle k_f \rangle$ (from 8 s^{-1} to ~14 s^{-1}) is just in the opposite direction of that predicted by the model, i.e., when the relative amplitude of the fast phase increases, its rate constant also increases. At high inhibition of k_{AB} and k_{BA}, the model also predicts a decrease in the rate constant of the residual slow recombination phase (Fig. A1, *C*), which is not observed in dehydrated trehalose glasses as compared to ''wet'' matrices (see Fig. 2 *C*).

On the basis of these marked discrepancies between the predicted (Fig. A1) and the experimentally observed inhibition pattern (Fig. 2) it is concluded that a progressive inhibition of Q_A^--to-Q_B electron transfer occurring homogeneously over the whole RC population is inconsistent with the recombination kinetics measured in dehydrated trehalose matrices.

SUPPLEMENTARY MATERIAL

An online supplement to this article can be found by visiting BJ Online at http://www.biophysj.org.

We thank Alejandro Hochkoeppler for assistance in NIR measurements, B. Andrea Melandri for critically reading the manuscript, and G. Cottone, P. Turina, and E. Vitrano for useful, stimulating discussions.

The financial support of Ministero dell'Istruzione, dell'Università e della Ricerca of Italy is acknowledged by F.F. and G.V. (grant PRIN/2001 ''Bioenergetica: aspetti genetici, biochimici e fisiopatologici''; grant FIRB/2001 ''Meccanismi Molecolari della Fotosintesi'') and by G.P. (grant PRIN/2001 ''Struttura e Dinamica di Sistemi a Grande Interfase''). G.P. was supported by the Consorzio Interuniversitario per lo sviluppo dei Sistemi a Grande Interfase (CSGI-Firenze).

REFERENCES

Ambrosone, L., A. Mallardi, G. Palazzo, and G. Venturoli. 2002. Effect of heterogeneity in the distribution of ligands and proteins among disconnected particles: the binding of ubiquinone to the bacterial reaction center. *Phys. Chem. Chem. Phys.* 4:3071–3077.

Arata, H., and W. W. Parson. 1981. Enthalpy and volume changes accompanying electron transfer from P-870 to quinones in *Rhodopseudomonas sphaeroides* reaction centers. *Biochim. Biophys. Acta.* 636:70–81.

Austin, R. H., K. W. Beeson, L. Eisenstein, H. Frauenfelder, and I. C. Gunsalus. 1975. Dynamics of ligand binding to myoglobin. *Biochemistry.* 14:5355–5373.

Baciou, L., and H. Michel. 1995. Interruption of the water chain in the reaction center from *Rhodobacter sphaeroides* reduces the rates of the proton uptake and of the second electron transfer to Q_B. *Biochemistry.* 34:7967–7972.

Balabin, I. A., and J. N. Onuchic. 2000. Dynamically controlled protein tunneling paths in photosynthetic reaction centers. *Science*. 290:114–117.

Barron, L. D., L. Hecht, and G. Wilson. 1997. The lubricant of life: a proposal that solvent water promotes extremely fast conformational fluctuations in mobile heteropolypeptide structure. *Biochemistry*. 36:13143–13147.

Beechem, J. M. 1992. Global analysis of biochemical and biophysical data. *Methods Enzymol*. 20:37–54.

Bevington, P. R. 1969. Data Reduction and Error Analysis for the Physical Sciences. McGraw-Hill, New York.

Breton, J., C. Boullais, C. Mioskowsky, P. Sebban, L. Baciou, and E. Nabedryk. 2002. Vibrational spectroscopy favors a unique Q_B binding site at the proximal position in wild-type reaction centers and in the Pro-L209→Tyr mutant from *Rhodobacter sphaeroides*. *Biochemistry*. 41:12921–12927.

Brzezinski, P., and L.-E. Andreasson. 1995. Trypsin treatment of reaction centers from *Rhodobacter sphaeroides* in the dark and under illumination: protein structural changes follow charge separation. *Biochemistry*. 34:7498–7506.

Careri, G. 1992. Proton percolation and emergence of function in nearly dry biosystems. *Nanobiology*. 1:117–126.

Cherepanov, D. A., L. I. Krishtalik, and A. Y. Mulkidjanian. 2001. Photosynthetic electron transfer controlled by protein relaxation: analysis by Langevin stochastic approach. *Biophys. J*. 80:1033–1049.

Cordone, L., P. Galajada, E. Vitrano, A. Gassmann, A. Ostermann, and F. Parak. 1998. A reduction of protein-specific motions in co-ligated myoglobin embedded in a trehalose glass. *Eur. Biophys. J*. 27:173–176.

Cordone, L., M. Ferrand, E. Vitrano, and G. Zaccai. 1999. Harmonic behavior of trehalose-coated carbon-monoxy-myoglobin at high temperature. *Biophys. J*. 76:1043–1047.

Cottone, G., L. Cordone, and G. Ciccotti. 2001. Molecular dynamics simulation of carboxy-myoglobin embedded in a trehalose-water matrix. *Biophys. J*. 80:931–938.

Cottone, G., G. Ciccotti, and L. Cordone. 2002. Protein-trehalose-water structures in trehalose coated carboxy-myoglobin. *J. Chem. Phys*. 117:9862–9866.

Crowe, L. M., D. S. Reid, and J. H. Crowe. 1996. Is trehalose special for preserving biomaterials? *Biophys. J*. 71:2087–2093.

Davidson, V. L. 1996. Unravelling the kinetic complexity of interprotein electron transfer reactions. *Biochemistry*. 45:14035–14039.

Edens, G. J., M. R. Gunner, Q. Xu, and D. Mauzerall. 2000. The enthalpy and entropy of reaction for formation of $P^+Q_A^-$ from excited reaction centers of *Rhodobacter sphaeroides*. *J. Am. Chem. Soc*. 122:1479–1485.

Feher, G., and M. Y. Okamura. 1978. Chemical composition and properties of reaction centers. *In* The Photosynthetic Bacteria. R. K. Clayton, and W. R. Sistrom, editors. Plenum Press, New York. pp.349–386.

Feher, G., M. Okamura, and D. Kleinfeld. 1987. Electron transfer reactions in bacterial photosynthesis: charge recombination kinetics as a structure probe. *In* Protein Structure. Molecular and Electronic Reactivity. R. Austin, E. Buhks, B. Chance, D. De Vault, P. L. Dutton, H. Frauenfelder, and V. I. Goldanskii, editors. Springer-Verlag, New York. pp.399–421.

Feher, G., J. P. Allen, M. Y. Okamura, and D. C. Rees. 1989. Structure and function of bacterial photosynthetic reaction centres. *Nature*. 33:111–116.

Frauenfelder, H., F. Parak, and R. D. Young. 1988. Conformational substates in proteins. *Annu. Rev. Biophys. Biophys. Chem*. 17:451–479.

Frauenfelder, H., S. G. Sligar, and P. G. Wolynes. 1991. The energy landscapes and motions of proteins. *Science*. 254:1598–1603.

Frauenfelder, H., and P. G. Wolynes. 1994. Biomolecules: where the physics of complexity and simplicity meet. *Phys. Today*. 47:58–64.

Frauenfelder, H., and B. McMahon. 1998. Dynamics and function of proteins: the search for general concepts. *Proc. Natl. Acad. Sci. USA*. 95:4795–4797.

Gottfried, D. S., E. S. Peterson, A. G. Sheikh, J. Wang, M. Yang, and J. M. Friedman. 1996. Evidence for damped hemoglobin dynamics in a room temperature trehalose glass. *J. Phys. Chem*. 100:12034–12042.

Graige, M. S., G. Feher, and M. Y. Okamura. 1998. Conformational gating of the electron transfer reaction $Q_A^-Q_B \rightarrow Q_AQ_B^-$ in bacterial reaction centers of *Rhodobacter sphaeroides* determined by a driving force assay. *Proc. Natl. Acad. Sci. USA*. 95:11679–11684.

Gray, K. A., J. W. Farchaus, J. Wachtveitl, J. Breton, and D. Oesterhelt. 1990. Initial characterization of site-directed mutants of tyrosine M210 in the reaction centre of *Rhodobacter sphaeroides*. *EMBO J*. 9:2061–2070.

Gunner, M. R. 1991. The reaction center protein from purple bacteria: structure and function. *Curr. Topics Bioenerg*. 16:319–367.

Hagen, S. J., J. Hofrichter, and W. A. Eaton. 1995. Protein reaction kinetics in a room-temperature glass. *Science*. 269:959–962.

Hagen, S. J., J. Hofrichter, and W. A. Eaton. 1996. Geminate rebinding and conformational dynamics of myoglobin embedded in a glass at room temperature. *J. Phys. Chem*. 100:12008–12021.

Hoffman, B. M., and M. A. Ratner. 1987. Gated electron transfer: when are observed rates controlled by conformational interconversion? *J. Am. Chem. Soc*. 109:6237–6242.

Holzwarth, A. R. 1996. Data analysis of time-resolved measurements. *In* Biophysical Techniques in Photosynthesis. J. Amesz, and A. J. Hoff, editors. Kluwer Academic Publishers, Dordrecht, The Netherlands. pp.75–92.

Izrailev, S., A. R. Crofts, E. A. Berry, and K. Shulten. 1999. Steered molecular dynamics simulation of the Rieske subunit motion in the cytochrome bc_1 complex. *Biophys. J*. 77:1753–1768.

Kalman, L., and P. Maroti. 1997. Conformation-activated protonation in reaction centers of the photosynthetic bacterium *Rhodobacter sphaeroides*. *Biochemistry*. 36:15269–15276.

Kirmaier, C., D. Holten, and W. W. Parson. 1985. Temperature and detection-wavelength dependence of the picosecond electron transfer kinetics measured in *Rhodopseudomonas sphaeroides* reaction centers. Resolution of new spectral and kinetic components in the primary charge separation process. *Biochim. Biophys. Acta*. 810:37–48.

Kleinfeld, D., M. Y. Okamura, and G. Feher. 1984a. Electron-transfer kinetics in photosynthetic reaction centers cooled to cryogenic temperatures in the charge-separated state: evidence for light-induced structural changes. *Biochemistry*. 23:5780–5786.

Kleinfeld, D., M. Y. Okamura, and G. Feher. 1984b. Electron transfer in reaction centers of *Rhodopseudomonas spheroides*. I. Determination of the charge recombination pathway of $D^+Q_AQ_B^-$ and free energy and kinetic relations between $Q_A^-Q_B$ and $Q_AQ_B^-$. *Biochim. Biophys. Acta*. 766:126–140.

Kotelnikov, A. I., V. R. Vogel, A. V. Pastuchov, V. L. Voskoboinikov, and E. S. Medvedev. 1998. Coupling of electron transfer and protein dynamics. *In* Biological Electron Transfer Chains: Genetic, Composition and mode of Operation. G. V. Canters, and E. Vijgenbom, editors. Kluwer Academic Publishers, Dordrecht, The Netherlands. pp.29–51.

Kuglstatter, A., U. Emler, H. Michel, L. Baciou, and G. Fritzsch. 2001. X-ray structure analyses of photosynthetic reaction center variants from *Rhodobacter sphaeroides*: structural changes induced by point mutations at position L209 modulate electron and proton transfer. *Biochemistry*. 40:4253–4260.

Labahn, A., J. M. Bruce, M. Y. Okamura, and G. Feher. 1995. Direct charge recombination from $D^+Q_AQ_B^-$ to DQ_AQ_B in bacterial reaction centers from *Rhodobacter sphaeroides* containing low potential quinone in the Q_A site. *Chem. Phys*. 197:355–366.

Leslie, S. B., E. Israeli, B. Lighthaert, J. H. Crowe, and L. M. Crowe. 1995. Trehalose and sucrose protect both membranes and proteins in intact bacteria during drying. *Appl. Environ. Microbiol*. 91:3592–3597.

Li, J., D. Gilroy, D. M. Tiede, and M. R. Gunner. 1998. Kinetic phases in the electron transfer from $P^+Q_A^-Q_B$ to $P^+Q_AQ_B^-$ and the associated processes in *Rhodobacter sphaeroides* R-26 reaction centers. *Biochemistry*. 37:2818–2829.

Li, J., E. Takahashi, and M. R. Gunner. 2000. $-\Delta G_{AB}^{o}$ and pH dependence of the electron transfer from $P^{+}Q_{A}^{-}Q_{B}$ to $P^{+}Q_{A}Q_{B}^{-}$ in *Rhodobacter sphaeroides* reaction centers. *Biochemistry*. 39:7445–7454.

Librizzi, F., E. Vitrano, and L. Cordone. 1999. Inhibition of A substates interconversion in trehalose-coated carbonmonoxy-myoglobin. *In* Biological Physics. H. Frauenfelder, G. Hummer, and R. Garcia, editors. American Institute of Physics, Melville, New York. pp.132–138.

Librizzi, F., C. Viappiani, S. Abbruzzetti, and L. Cordone. 2002. Residual water modulates the dynamics of the protein and of the external matrix in ''trehalose-coated'' MbCO: an infrared and flash-photolysis study. *J. Chem. Phys*. 116:1193–1200.

Lieutaud, C., W. Nitschke, A. Verméglio, P. Parot, and B. Schoepp-Cothenet. 2003. HiPIP in *Rubrivivax gelatinosus* is firmly associated to the membrane in a conformation efficient for electron transfer towards the photosynthetic reaction centre. *Biochim. Biophys. Acta*. 1557:83–90.

Mallardi, A., G. Palazzo, and G. Venturoli. 1997. Binding of ubiquinone to photosynthetic reaction centers: determination of enthalpy and entropy changes in reverse micelles. *J. Phys. Chem. B*. 101:7850–7857.

Mancino, L. J., D. P. Dean, and R. E. Blankenship. 1984. Kinetics and thermodynamics of the $P870^{+}\ Q_{A}^{-} \rightarrow P870^{+}Q_{B}^{-}$ reaction in isolated reaction centers from the photosynthetic bacterium *Rhodopseudomonas sphaeroides*. *Biochim. Biophys. Acta*. 764:46–54.

Mattos, C. 2002. Protein-water interactions in a dynamic world. *Trends Biochem. Sci*. 27:203–208.

McMahon, B. H., J. D. Müller, C. A. Wraight, and G. U. Nienhaus. 1998. Electron transfer and protein dynamics in the photosynthetic reaction center. *Biophys. J*. 74:2567–2587.

Nabedryk, E., K. A. Bagley, D. L. Thibodeau, M. Bausher, W. Mäntele, and J. Breton. 1990. A protein conformational change associated with the photoreduction of the primary and secondary quinones in the bacterial reaction center. *FEBS Lett*. 266:59–62.

Okamura, M. Y., M. L. Paddock, M. S. Graige, and G. Feher. 2000. Proton and electron transfer in bacterial reaction centers. *Biochim. Biophys. Acta*. 1458:148–163.

Ortega, J. M., P. Mathis, J. C. Williams, and J. P. Allen. 1996. Temperature dependence of the reorganization energy for charge recombination in the reaction center from *Rhodobacter sphaeroides. Biochemistry*. 35:3354–3361.

Paddock, M. L., S. H. Rongey, G. Feher, and M. Y. Okamura. 1989. Pathway of proton transfer in bacterial reaction centers: replacement of glutamic acid 212 in the L-subunit by glutamine inhibits quinone (secondary acceptor) turnover. *Proc. Natl. Acad. Sci. USA*. 86:6602–6606.

Palazzo, G., A. Mallardi, M. Giustini, D. Berti, and G. Venturoli. 2000. Cumulant analysis of charge recombination kinetics in bacterial reaction centers reconstituted into lipid vesicles. *Biophys. J*. 79:1171–1179.

Palazzo, G., A. Mallardi, A. Hochkoeppler, L. Cordone, and G. Venturoli. 2002. Electron transfer kinetics in photosynthetic reaction centers embedded in trehalose glasses: trapping of conformational substates at room temperature. *Biophys. J*. 82:558–568.

Parot, P., J. Thiery, and A. Vermeglio. 1987. Charge recombination at low temperature in photosynthetic bacteria reaction centers: evidence for two conformational states. *Biochim. Biophys. Acta*. 893:534–543.

Peloquin, J. M., J. C. Williams, X. Lin, R. G. Alden, A. K. W. Taguchi, J. P. Allen, and N. W. Woodbury. 1994. Time-dependent thermodynamics during early electron transfer in reaction centers from *Rhodobacter sphaeroides*. *Biochemistry*. 33:8089–8100.

Sharp, R. E., and S. K. Chapman. 1999. Mechanisms for regulating electron transfer in multi-centre redox proteins. *Biochim. Biophys. Acta*. 1432:143–158.

Shopes, R. J., and C. A. Wraight. 1985. The acceptor quinone complex of *Rhodopseudomonas viridis* reaction centers. *Biochim. Biophys. Acta*. 806:348–356.

Stowell, M. H. B., T. M. McPhillips, D. C. Rees, S. M. Soltis, E. Abresch, and G. Feher. 1997. Light-induced structural changes in photosynthetic reaction center: implication for mechanism of electron-proton transfer. *Science*. 276:812–816.

Takahashi, E., and C. A. Wraight. 1992. Proton and electron transfer in the acceptor quinone complex of *Rhodobacter sphaeroides* reaction centers: characterization of site-directed mutants of the two ionizable residues, *Glu*L212 and *Asp*L213, in the Q_{B} binding site. *Biochemistry*. 31:855–866.

Tiede, D. M., J. Vázquez, J. Córdova, and P. A. Marone. 1996. Time-resolved electrochromism associated with the formation of quinone anions in the *Rhodobacter sphaeroides* R26 reaction center. *Biochemistry*. 35:10763–10775.

Tiede, D. M., L. Utschig, D. K. Hanson, and D. M. Gallo. 1998. Resolution of electron and proton transfer events in the electrochromism associated with quinone reduction in bacterial reaction centers. *Photosynth. Res*. 55:267–273.

Uritani, M., M. Takai, and K. Yoshinaga. 1995. Protective effect of disaccharides on restriction endonucleases during drying under vacuum. *J. Biochem*. 117:774–779.

Van Mourik, F., M. Reus, and A. R. Holzwarth. 2001. Long-lived charge-separated states in bacterial reaction centers isolated from *Rhodobacter sphaeroides*. *Biochim. Biophys. Acta*. 1504:311–318.

Vermeglio, A., and R. K. Clayton. 1977. Kinetics of electron transfer between the primary and the secondary electron acceptor in reaction centers from *Rhodopseudomonas sphaeroides*. *Biochim. Biophys. Acta*. 461:159–165.

Vitkup, D., D. Ringe, G. A. Petsko, and M. Karplus. 2000. Solvent mobility and the protein ''glass'' transition. *Nat. Struct. Biol*. 7:34–38.

Walden, S. E., and R. A. Wheeler. 2002. Protein conformational gate controlling binding site preference and migration for ubiquinone-B in the photosynthetic reaction center of *Rhodobacter sphaeroides*. *J. Phys. Chem. B*. 106:3001–3006.

Woodbury, N. W. T., and W. W. Parson. 1984. Nanosecond fluorescence from isolated photosynthetic reaction centers of *Rhodopseudomonas sphaeroides*. *Biochim. Biophys. Acta*. 767:345–361.

Woodbury, N. W. T., and W. W. Parson. 1986. Nanosecond fluorescence from chromatophores of *Rhodopseudomonas sphaeroides* and *Rhodospirillum rubrum. Biochim. Biophys. Acta*. 850:197–210.

Xu, Q., and M. R. Gunner. 2001. Trapping conformational intermediate states in the reaction center protein from photosynthetic bacteria. *Biochemistry*. 40:3232–3241.

Xu, Q., and M. R. Gunner. 2002. Exploring the energy profile of the Q_{A}^{-}-to-Q_{B} electron transfer reaction in bacterial photosynthetic reaction centers: pH dependence of the conformational gating step. *Biochemistry*. 41:2694–2701.

Xu, Q., L. Baciou, P. Sebban, and M. R. Gunner. 2002. Exploring the energy landscape for Q_{A}^{-}-to-Q_{B} electron transfer in bacterial photosynthetic reaction centers: effect of substrate position and tail length on the conformational gating step. *Biochemistry*. 41:10021–10025.

Zhang, Z., L. Huang, Y.-I. Chi, K. K. Kim, A. R. Crofts, E. A. Berry, and S.-H. Kim. 1998. Electron transfer by domain movement in cytochrome bc_{1}. *Nature*. 392:677–684.